JAERI-Tech
95-016

STUDY ON THE PHOTOACOUSTIC SPECTROSCOPY CAPABILITIES WITH REMOTE DETECTION FOR MONITORING OF ACTINIDE SPECIES IN NUCLEAR FUEL REPROCESSING SOLUTIONS

March 1995

Sergey I. SINKOV*, Takehiro KIHARA
Sachio FUJINE and Mitsuru MAEDA

日本原子力研究所
Japan Atomic Energy Research Institute

本レポートは，日本原子力研究所が不定期に公刊している研究報告書です。
入手の問合わせは，日本原子力研究所技術情報部情報資料課（〒319-11 茨城県那珂郡東海村）あて，お申し越しください。なお，このほかに財団法人原子力弘済会資料センター（〒319-11 茨城県那珂郡東海村日本原子力研究所内）で複写による実費頒布をおこなっております。

This report is issued irregularly.
Inquiries about availability of the reports should be addressed to Information Division, Department of Technical Information, Japan Atomic Energy Research Institute, Tokai-mura, Naka-gun, Ibaraki-ken 319-11, Japan.

編集兼発行　日本原子力研究所
印　　刷　㈱高野高速印刷

Study on the Photoacoustic Spectroscopy Capabilities with Remote Detection for Monitoring of Actinide Species in Nuclear Fuel Reprocessing Solutions

Sergey I. SINKOV*, Takehiro KIHARA, Sachio FUJINE and Mitsuru MAEDA

Department of Fuel Cycle Safety Research
Tokai Research Establishment
Japan Atomic Energy Research Institute
Tokai-mura, Naka-gun, Ibaraki-ken

(Received February 6, 1995)

A LIPAS (Laser Induced Photoacoustic Spectroscopy) system has been developed for remote analysis of weakly absorbing species in solution. A number of photoacoustic cells of various configurations have been examined in remote arrangement of PA spectrometer with application of an optical fiber for the laser light transmission to PA cell.

A microscope objective was tested in optical fiber launching arrangement to collimate laser beam after the fiber. It has been shown that short optical pathlengh cuvette type cells in combination with a disk type piezoelectric transducer (PZT) are superior to previously used cylindrical PA cell with a tube type PZT as regards more effective elimination of scattered and reflected light contribution to PZT response. This allows to improve the linearity of calibration curve and to lower the detection limit absorptivity down to 4.2×10^{-5} cm^{-1}, which has been evaluated using an absorption band of Nd at 511.4 nm.

The newly designed PA cell has been applied for investigation of PAS capabilities to detection of Pu(Ⅲ), Pu(Ⅳ) and Pu(Ⅵ) simulated species in uranium containing solutions relevant to the nuclear fuel reprocessing technology. It has been shown that the proper selection of plutonium absorption band for each oxidation state allows to reduce high background contribution from U(Ⅵ) ions to the analytical PA signal and to keep detection limit absorptivity within a 1-3 $\times10^{-5}$ cm^{-1} range in the 525-562 nm wavelength region.

Keywords : Laser, Photoacoustic Spectroscopy, Actinides, Speciation, Optical Fiber

* Research Fellow

再処理溶液中アクチノイドの遠隔分析のための光音響分光法に関する研究

日本原子力研究所東海研究所燃料サイクル安全工学部
Sergey I. SINKOV*・木原　武弘・藤根　幸雄・前田　　充

（1995年2月6日受理）

溶液中微弱吸収種の遠隔分析のため，LIPAS（レーザー誘起光音響分光法）システムを開発した。セルへの光の誘導には光ファイバーを応用し，様々な形状の光音響（ＰＡ）セルを試験した。

ファイバー出射後の集光に，対物レンズを試した。散乱光の圧電素子（ＰＺＴ）に与える影響を効果的に小さくするには，短い光路長の角型セルと円盤型のＰＺＴの組み合わせの方が，前研究での円筒型セルと円筒型ＰＺＴとの組み合わせより優れていることが分かった。Ｎｄの511.4nmの吸収を用いた試験で，検量線の直線性は良く，検出限界は$4.2\times10^{-5}cm^{-1}$であった。

新しくデザインしたＰＡセルを再処理工程におけるウラン溶液中のＰｕ分析への応用のため，Ｐｕ（Ⅲ），Ｐｕ（Ⅳ）及びＰｕ（Ⅵ）の模擬物質を分析した。それぞれの酸化状態のＰｕ吸収を適切に選択することにより，ウランからの高いバックグラウンド信号を小さくすることができ，525～562nmの１～３$\times10^{-5}cm^{-1}$を示すことが分かった。

東海研究所：〒319－11　茨城県那珂郡東海村白方字白根２－４
*　リサーチフェロー

Contents

目　　次

1. INTRODUCTION

Photoacoustic spectroscopy (PAS) of aqueous solutions is widely used as a new elegant tool for nondestructive chemical analysis capable, in particular, of detection and identification of rare earth , actinide and some fission product species at a micromolar concentration level [1–3]. Its sensitivity is several hundred times higher than that of conventional spectrophotometry.

The creation of the photoacoustic (PA) signal is based on the conversion of absorbed optical radiation (laser pulse) into heat by nonradiative relaxation processes. The transuranium ions and solvent molecules release the absorbed energy to the solution, which is heated locally in the volume illuminated by the laser pulse and consequently expands. This generates a compression wave with an amplitude proportional to the absorbance of the solute. Starting from the point of origination, the wave propagates radially through the solution and is detected by a piezoelectric transducer (PZT), which converts the energy of compression wave into an electrical signal. Other energy release processes such as fluorescence and phosphorescence do not contribute directly to the creation of photoacoustic signal. The magnitude of PA signal depends from absorption characteristics of a solvent and a solute and it is proportional to the concentration of analyte in the range of applicability of the Beer's law.

Although many papers have been published on photoacoustic spectroscopy application to speciation of actinides and rare earth elements, practically all of them refer to aqueous solution containing no other macrocomponents than water and mineral acid or to aquatic systems with humic acid as naturally occurring complex forming reagent. No research has been reported on PAS application to nuclear fuel reprocessing solutions, which usually contain U(VI) and/or U(IV) as the main background components contributing greatly to overall absorption level of solution in a wide range of absorption spectrum of aqueous phase. This may impose serious limitations on PAS applicability to determination of various valent states of heavier actinides, among which the plutonium speciation is especially important mainly due to its diverse redox chemistry and demand to control carefully its pathways at various stages of nuclear fuel reprocessing. Pu may occur in solution in various oxidation states, which often coexist with each other. Although Pu(IV) is the predominant valent form of this element after nuclear fuel dissolution, Pu(III) and Pu(VI) should not be excluded from consideration even after the plutonium valency adjustment to tetravalent state.

On the other hand, uranium itself is also an important component to be controlled in reprocessing solution even when its concentration decreases down to submillimole level, when application of conventional spectrophotometry may be not effective. One of important tasks relevant to this problem is a need to control the remaining concentration of U(IV) in aqueous phase of battery B in PUREX process after Pu back–extraction from organic phase as result of its reduction by U(IV). In this case the problem is to measure U(IV) as a minor component in the presence of much larger amounts of Pu(III) as a background species.

Application of PAS for research in nuclear fuel reprocessing requires protection of laser equipment and detection electronics from probable radiation damage. Usually these facilities are surrounded by a heavy concrete wall, therefore, remote PA detection is needed. This problem can be solved through a spatial separation of PA cell from the excitation and registration parts of PA spectrometer, keeping them outside of high radiation area. The laser light transmission from the laser to PA cell can be performed by using an optical fiber of appropriate length as a light guide.

This research project has been aimed at development of photoacoustic spectrometer for sensitive analysis of weakly absorbing species of actinide elements in solutions relevant to the nuclear fuel reprocessing technology. This spectrometer should meet the following requirements:

1) high sensitivity of PA cell allowing to attain detection limit absorptivity of $n \times 10^{-5}$ cm^{-1} (n=1–3), which is reported to be achieved by several research groups from USA and Europe;

2) possibility of remote detection of the species under study by means of laser light transmission from laser the the cell through an optical fiber;

3) effective discrimination of PA signal originated from the species of interest against background absorption of the matrix components to keep the detection limit within the range indicated in item 1)

The work described in this report can be divided onto three main parts:

1) solution of the problem of poor linearity of calibration curve for the cylindrical long pathlength flowthrough cell appearing in case of laser pulse transmission through an optical fiber;

2) optimization of new configuration of PA cell based on a rectangular cuvette spectrophotometric cell in combination with a disk type PZT;

3) application of PAS technique for detection of tri–, tetra– and hexavalent plutonium simulated species in uranium containing solution relevant to nuclear fuel cycle.

2. EXPERIMENTAL

A UV-160A Shimadzu spectrophotometer was used for recording of optical absorption spectra of analytes and background components in a high (0.05–2.0 cm^{-1}) absorptivity range.

2.1 PA cell and piezoelectric transducer

A flowthrough cylindrical PA cell with the optical pathlength of 100 mm and a coaxial tube type PZT, decribed in detail in [4, 5], has been examined in this research with an optical fiber launching arrangement.

Three cuvette type spectrophotometric cells with rectangular cross section and optical pathlength of 10 and 20 mm (Fig. 1) have been tested in combination with a disk type PZT of various diameter and thickness as a novel configuration of PA cell in the laboratory. The main reason of the cuvettes choice was their commercial availability and simple configuration suitable for attachment of the transducer from an external side of the cell to avoid corrosion of PZT.

2.2 PA spectrometer with remote arrangement

A block diagram of the PA spectrometer with remote detection is shown in Fig.2. A Nd:YAG laser with a repetition rate of 10 Hz was used to pump a TDL-50 dye laser. Two Coumarin dyes (C-480 and C-500) were used to cover a wavelength range from 465 to 533 nm; F548 dye was used in the 545–569 nm range overlapping the absorption maxima of Pu(IV) at 550 nm and Pu(III) at 562 nm. Laser beam energy varied from 0.5 to 12 mJ depending on the generation efficiency and gain profile of a particular dye. A neutral density filter set was used to attenuate the output pulse energy of the dye to a desired level.

A 2-m airtight optical fiber (ST 1200I-SY, Mitsubishi Cable Industries, LTD) made from silica glass with a core diameter of 1.2 mm was used for the laser light transmission. The losses in the fiber according to manufacturer`s information do not exceed 20 dB/km at 850 nm and fiber`s damage threshold was calculated to be not lower than 8 mJ for given core diameter and laser pulse duration of 9 ns.

Two possibilities of laser beam introduction into the cell were examined: a collimated beam propagation and non collimated beam propagation

In the first case at the remote end of fiber, a x3.3 two lens microscope objective was used to collimate the output laser beam and direct it into a cuvette containing a sample solution. The objective was placed 3 cm from the fiber which produced a quazi collimated beam approximately 3.5 mm in diameter for the first 10 cm of its propagation.

In case of non collimated beam propagation the laser beam exiting the fiber as a diverging cone of light was launched directly into the cell without any other optical components (see Fig. 3

for illustration)

The photoacoustic cell assembly was placed within a thin wall stainless steel container with small holes for laser beam propagation to eliminate the external electromagnetical noise.

The signal from PZT was amplified by a NF5305 amplifier followed by a NF FV-628B wide range decade filter to provide the low- and high frequency cut-off borders below 160 kHz and above 260 kHz. A PM 3320A digital storage oscilloscope was used for measurement and processing of the conditioned PA signal after selection of the most intensive peak in the initial part of a transient signal and verification of its linear concentration dependence.

A pin-hole photodiode (Gentec, ED-100A) in combination with a 50 mm plano-convex focusing lens was used as a light trap to collect a beam exiting the cuvette. The photodiode monitored the laser energy in order to take into account pulse to pulse energy fluctuations and to ratio the measured PA spectrum to a dye wavelength power profile. The signal from the photodiode was recorded using a boxcar integrator (BX-531, NF Sci. Instr.).

2.3 Reagents for preparation of the background and analyte solutions

A stock solution of U(VI) with U concentration of 100 g/l was used for preparation of working solutions by its dilution by 3N nitric acid. Solution of U(VI) in 30% TBP in n-dodecane was obtained by extraction of U(VI) from aqueous phase. The efficiency of extraction was controlled by recording absorption spectrum of aqueous phase after extraction and it was found to be more than 98%.

Solutions of Nd(III) and Pr(III) ions were prepared by dissolution of their nitrates in purified water and their concentration was determined by ICP-AES analysis. They were used for demonstration of PA spectrometer performance in the 465 -533 nm range

As it was not possible to use the real plutonium solutions for PAS application, the following substituents were used to imitate its various oxidation states: absorption band of Pr(III) at 481.3 nm as imitation of Pu(IV) absorption at 480 nm; a 522 nm peak of Nd(III) to imitate a 525 nm peak of Pu(VI); broad absorption band of Cr(III) ion covering peaks of Pu(IV) at 550 nm and Pu(III) at 562 nm. All the reagents proved to be compatible with background solution of U(VI), i.e. no changes in physical properties of solution after the analyte introduction were observed (precipitation, distortion of background absorption spectra, etc.)

2.4 Modified sample preparation procedure for PAS calibration experiment

An advanced sample preparation procedure has been applied for the first time in the practice of PA calibration experiment which is based on creation of concentration series of solutions directly in a PA cell. A mathematical description has been developed to derive the correction coefficients accounting for concentrational changes of an analyte as result of solution volume adjustment in the cell from one concentration point to another.

Detailed description of this routine is given in Appendix 1 and some results on calculation of correction coefficients are shown in Table 1.

No negative effect of the solution agitation used to provide a uniform distribution of new portion of analyte within the working volume of cuvette on the PA signal perturbation was observed 3 min after completion of the sample preparation. The main advantage of this approach is a possibility to perform the calibration experiment handling much less quantity of the analyte and total volume of solution and, therefore, to reduce significantly the amount of waste accumulated after the calibration experiment, which is very important for operation with highly radioactive, hazardous and/or expensive analytes.

3. RESULTS AND DISCUSSION

3.1 Comparison a long pathlength cylindrical PA cell characteristics in direct laser beam introduction mode and in remote arrangement.

The flowthrough cylindrical PA cell with the optical pathlength of 100 mm and a coaxial tube type PZT had been designed and successfully tested in the Process Engineering Laboratory of JAERI several years ago and it was further applied for detection of some rare earth elements and Np(V) in aqueous solutions at the wavelengths generated by the Rhodamine dyes pumped by the second harmonics of Nd(YAG) laser (532 nm), i.e in the range from 565 nm to 640 nm [4,5]. That time the researchers achieved detection limit absorptivity of 3.3×10^{-5} cm^{-1}. This section describes some results of evaluation of the cell detection limit in the range of Coumarine-500 dye laser generation (494 - 533 nm) using several laser beam launching arrangements. This dye is pumped by the third harmonics of Nd(YAG) laser (355 nm), which results in more narrow beam diameter and not so uniform beam profile as in the former case.

3.1.1 Direct laser beam introduction into the cell

An absorption peak of Nd(III) ions in aqueous solution at 511.4 nm was used for investigation of calibration curve linearity and assessment of sensitivity and detection limit of the cell. After elimination of large background signal caused by a non-tunable amplified spontaneous emission by using an iris to avoid generation of PA signal in the front part of the cell container, a good linearity of calibration curve was obtained , but the detection limit was not as low as expected (1×10^{-4} cm^{-1}). An additional bandpass filter was used after the second amplifier of PA signal to reduce the high frequency noise constituent of PZT which allowed to attain detection limit of 3.9×10^{-5} cm^{-1}.

Detailed description of this routine is given in Appendix 1 and some results on calculation of correction coefficients are shown in Table 1.

No negative effect of the solution agitation used to provide a uniform distribution of new portion of analyte within the working volume of cuvette on the PA signal perturbation was observed 3 min after completion of the sample preparation. The main advantage of this approach is a possibility to perform the calibration experiment handling much less quantity of the analyte and total volume of solution and, therefore, to reduce significantly the amount of waste accumulated after the calibration experiment, which is very important for operation with highly radioactive, hazardous and/or expensive analytes.

3. RESULTS AND DISCUSSION

3.1 Comparison a long pathlength cylindrical PA cell characteristics in direct laser beam introduction mode and in remote arrangement.

The flowthrough cylindrical PA cell with the optical pathlength of 100 mm and a coaxial tube type PZT had been designed and successfully tested in the Process Engineering Laboratory of JAERI several years ago and it was further applied for detection of some rare earth elements and Np(V) in aqueous solutions at the wavelengths generated by the Rhodamine dyes pumped by the second harmonics of Nd(YAG) laser (532 nm), i.e in the range from 565 nm to 640 nm [4,5]. That time the researchers achieved detection limit absorptivity of 3.3 x 10^{-5} cm^{-1}. This section describes some results of evaluation of the cell detection limit in the range of Coumarine-500 dye laser generation (494 - 533 nm) using several laser beam launching arrangements. This dye is pumped by the third harmonics of Nd(YAG) laser (355 nm), which results in more narrow beam diameter and not so uniform beam profile as in the former case.

3.1.1 Direct laser beam introduction into the cell

An absorption peak of Nd(III) ions in aqueous solution at 511.4 nm was used for investigation of calibration curve linearity and assessment of sensitivity and detection limit of the cell. After elimination of large background signal caused by a non-tunable amplified spontaneous emission by using an iris to avoid generation of PA signal in the front part of the cell container, a good linearity of calibration curve was obtained , but the detection limit was not as low as expected (1x 10^{-4} cm^{-1}). An additional bandpass filter was used after the second amplifier of PA signal to reduce the high frequency noise constituent of PZT which allowed to attain detection limit of 3.9 x 10^{-5} cm^{-1}.

3.1.2 An optical fiber launching arrangement with the laser beam collimation

It has been shown earlier that the use of a single focusing lens does not allow to launch laser beam from output end of fiber into a long path type PA cell effectively mainly due to high divergence of laser beam while its propagation along the optical pathlength of the cell. To avoid hitting of cell walls and a metal housing by the widening parts of direct laser radiation it was necessary to use an iris to cut the outer part of a laser beam spot before its entering the cell and, therefore, to inevitably reduce the total amount of laser energy. The first calibration curve referring to that case also contained concentration independent part of PA signal up to n x 10^{-3} cm^{-1} absorptivity values indicating on the background problem due to effect of illumination of PZT by the reflected light. Lack of linearity of calibration curve [5] led to the worsening of detection limit up to 2.5 x 10^{-3} cm^{-1}.

As one can judge from literature survey only one paper has been published up to date [6] dealing with application of optical fiber to development of remote PA detection in solution. The authors reported about a possibility to use a x10 microscope objective for launching laser light from fiber to PA cell to provide a collimated beam with diameter of 6 mm for a 10 cm optical path distance. No other technical details of this approach were given, that is why it has been decided to carry out some experiments with various types of microscope objectives to understand better the beam distance–cross section dependence after the output from objective and to verify an applicability of this arrangement to a longer optical path cell with a tube type PZT.

Preliminary tests had shown that among x2, x5, x10 objectives the x5 one possesses the most favorable characteristics allowing to use the full area of the laser beam spot from optical fiber and to produce a quasi collimated beam for the first 100 mm of its propagation path with a diameter range from 4.5 to 6.5 mm. This made it possible to position the PA cell with respect to a beam without hitting its inner side wall surface and PZT. At the input end of optical fiber a +120 mm focusing lens was used to collimate laser beam for its more efficient introduction into the fiber. The input end of fiber was positioned at the distance of 150 mm from lens, i.e. 30 mm behind its focus point. Total transmission efficiency of this arrangement, i.e. ratio of input energy before the fiber to its value behind the cell has been found to be 65%, being mainly the result of Freshel losses at every stage of beam propagation through optical surfaces.

The results of calibration experiment gave the detection limit of 3.1 x 10^{-4} cm^{-1} . On one hand, it is much better than obtained one year ago (2.5 x 10^{-3} cm^{-1}) for the case of beam collimation by a single lens, but, on the other hand, this value is still one order higher in comparison with the direct beam introduction. No clear linear dependence of PA signal versus absorptivity is observed for the lower part of calibration curve. The explanation of this peculiarity may be connected with reflection of a small portion of laser energy from the rear

window of PA cell back into the middle part of cell as a widening cone of light that can cause additional PZT response as result of its illumination. No such problem arises in case of direct introduction of laser beam to the cell because a divergence of the primary laser beam is much lower in comparison with its cross section variation after output from the objective.

3.1.3 Laser beam transmission through a quartz rod

An optical quality quartz rod (300 mm length, 3 mm diameter) has been tested also as an alternative to optical fiber for laser light transmission to PA cell. No additional collimation was used for the beam introduction into the rod body thanks to its larger diameter in comparison with the fiber. Almost immediately after starting laser beam adjustment for its collinear propagation along the central axis of the rod a narrow track of damage quartz medium was detected visually from the side view, the distance from input end of rod being equal to 50 mm and track length about 4 mm. After this accident a 50% neutral density filter was inserted across the laser beam way to reduce the input amount of energy for a safer operation with the quartz rod. Fortunately, the rod cross-section had enough area to readjust laser beam so as to avoid its propagation through the damaged area.

After that another problem have been discovered, namely, very strong self collimation of the central part of the beam profile at the output end of quartz rod. The local light intensity was so high that it caused a point size optical burn of the lens coating when the output laser beam was collimated using a single lens x 2 microscope objective. Finally the combination of two x1 single lens objectives in series has been found to be the most appropriate option to provide a quasi collimated beam propagation with beam diameter of 3.5 mm for the middle part of PA cell. Detection limit absorptivity for this arrangement is 1.02×10^{-4} cm^{-1}.

3.2 Development of a short optical pathlength PA cell

3.2.1 Preliminary experiments

Two sets of disk type PZTs became available soon after starting the research project, which varied in diameter: 10 and 20 mm. Each set, in turn, consisted of five PZTs differing in thickness: 3, 4, 5, 6, 7 and 8 mm.

For preliminary test experiments described in this section a 3mm x 10mm PZT was chosen. The problem of attachment of PZT to a cuvette cell was solved using a sliding bench of an optical rail holder which fitted well for this purpose. PZT was covered by a thin layer of the Apiezon grease to provide a better acoustic contact between transducer and bottom part of a quartz cell and, moreover, a thin aluminium foil was put between a cell bottom and the upper surface of PZT to minimize the effect of scattered light on PZT response.

Three types of spectrophotometric cell (all made from quartz) have been tested: a standard 45 x 10 x 10 mm cuvette cell with a round corner bottom, flowthrough rectangular type cell of the same external dimensions and volume of 3.2 cm^3 with nozzles oriented perpendicular to the optical walls and a micro flowthrough cell with at least twice smaller volume and nozzles lined up along the flow direction (Fig. 1 a, b, c).

First of all, a standard cuvette type PA cell (Fig. 1a) was tested to investigate its frequency response in order to select proper low and high frequency cut-off window borders for the bandpass filter. It has been shown that the optimal frequency window lies within a 160 – 260 kHz range. Preliminary experiments with Nd(III) solution at 511.4 nm have shown that it is very important to keep solution volume constant for comparison of various data, especially when performing absorption calibration experiment. Another important parameter strongly influencing the amplitude of PAS signal for a given absorbance value is a vertical laser beam position with respect to the bottom of the cell. Fig. 4, 5 present these vertical profiles of PA signal for two different amount of solution. All further experiments were carried out after preliminary adjustment of PA cell to position corresponding to the highest level of PA signal. The detection limit absorptivity have been found to be 2.6 x 10^{-5} cm^{-1} (solution volume is 2.5 cm^3).

A similar set of experiments was performed further for a rectangular flowthrough cell (Fig.1b). Fig. 6 presents a vertical profile of PA signal. The calibration experiment yielded a detection limit of 2.0 x 10^{-5} cm^{-1}, which is a little better than that for a standard cell. Therefore, this flowthrough cell can be successfully applied for PAS experiments with weakly absorbing solutions and it is more preferable for these studies because there is no need to control the solution volume and to take special measures to prevent a solution evaporation and its dust contamination.

Finally, a micro flowthrough quartz cell (Fig.1c) has been tested to evaluate its applicability and detection limit. A special small size holder was fabricated to provide an attachment of PZT to the side wall of the cell. There was fewer possibility to find out an optimal cell position with respect to laser beam due to small area of a polished cell window suitable for the laser beam introduction. Nevertheless, this cell has also exhibited good characterictics for PAS studies with detection limit being equal to 1.4 x 10^{-5} cm^{-1}.

After completion of these tests using a direct laser beam introduction the comparative experiment was carried out using an optical fiber for laser energy transmission to the rectangular flowthrough cell. A x3.3 microscope objective was used for collimation of laser beam after its exit from a distal end of the fiber which provided the resulting beam diameter of about 4 mm before entering the cell. No attempts were made to apply the full energy of dye laser beam to a light guide in order to avoid a damage of the fiber, that is why the amount of energy that reached PA cell did not exceed 0.35 mJ. This reduced energy caused additional

scattering of experimental data around their mean values, but linearity of calibration curve was good and detection limit was estimated to be equal 4.16 x 10^{-5} cm^{-1}. This value is 7 times better than that of obtained in experiments with a long path cell and a tube type PZT indicating that no problem connected with scattered and reflected light illumination of PZT appeared in the case of short pathlength flowthrough cell (Fig. 1b).

The results of preliminary tests of rectangular quartz cells with a disk type PZT have shown that these short pathlength PA cells possess good sensitivity, require much less amount of solution for PA detection of solute absorbance, allow to minimize effect of scattered light on PZT response in case of a poorly collimated beam propagation and can be successfully applied for PAS studies of weak absorbances including remote PA detection.

A photoacoustic spectrum of Nd(III) aqueous solution was measured after optimization of experimental configuration using a 0.2 mm increment wavelength scanning, which is presented in Fig. 7. The band at 511.4 nm has a molar absorptivity of only 1.79 l/mol cm^{-1}, while the adjacent one at 521.4 nm is characterized by 3.96 l/mol cm^{-1} value. This corresponds to absolute absorbance value of 3.76 x 10^{-4} cm^{-1} at 511.4 nm for a given concentration. Absorptivity of water in the selected spectral region is approximately 2 x 10^{-4} cm^{-1}. A comparison of the last two values with the ratio of the peak height in terms of PA signal level at 511.4 nm to that of the valley region at shorter wavelengths (505–510 nm) shows negligible contribution of the scattered laser light to PZT response and proves the efficiency of developed optical configuration in this respect.

Fig. 7 contains also a conventional absorption spectrum of the same species for a 500 times higher concentration of the solute. From the first glance, both spectra look quite similar as regards the peak positions and their relative intensities. But more detailed consideration reveals that the peak widths and a wavelength distance between the peaks are narrower than that of conventional spectrum. One of the plausible reasons for this distortion is discussed in Appendix 2.

3.2.2 A 10 x 10 x 45 mm (length x width x height) cell characteristics in combination with a PZT from a n x 10 mm set (n = 3, 4, 5, 6, 7, 8 mm).

All previously decribed data on a rectangular type PA cell characteristics with a disk type PZT referred to one particular PZT (thickness of 3 mm and diameter of 10 mm). The following four sections summarize the results of comparative tests of three rectangular quartz cells differing in their geometrical configuration (Fig.1 a, b, c) coupled to various PZT elements from the 10 mm and 20 mm diameter PZT sets. All experiments described here were performed using direct laser beam introduction into a PA cell (without an optical fiber launching arrangement).

A n x 10 mm diameter set included 6 pieces of PZT from 3 mm to 8 mm in thickness. The procedure of attachment of PZT to a standard cell (Fig. 1a) has been described earlier. After assembling a PA cell was placed within a noise–shielding container and positioned on a Y–Z

translation stage for a fine adjustment of the cell position with respect to the incident laser beam. In all these experiments solution volume was kept 2.5 ml. First step of optimization was connected with the search for an optimal beam height position corresponding to the most intensive PA signal for a given solution containing absorbing species. After the height has been optimized a frequency response of a PA cell was investigated using a band-pass filter scanning procedure with a narrow (10 kHz) gate between the low and high frequency cut-off borders. The results of this research are presented on the Fig.8. As it follows from these data, all six curves show well defined maxima obviously corresponding to the main resonance of PA cell assembly, and frequency positions of these maxima depend from the thickness of PZT with a gradual shift to a lower frequency for a thicker PZT element. As regards the PZT sensitivity, it increases with the thickness of a PZT from 3 to 6 mm (with a little exception for a 5 mm element) and remains almost the same for 6, 7 and 8 mm thick transducers.

Finally, each cell-PZT combination was tested in a calibration curve experiment using a number of Nd(III) solutions of various concentrations, that has allowed to evaluate more reliably the sensitivity of a PA cell as a slope of calibration curve and a noise level of PZT detector in the optimal frequency range of 100 kHz width. These results are presented in Table 2. This table includes also (although not directly) such characteristics as a standard deviation of PA signal of blank solution, a least-square deviation of experimental points from their theoretical values and a general standard deviation, which is calculated as a square root from the average value of variances for all experimental points. The comparison of the last two variances is often used in mathematical statistics to verify the validity of the assumed functional dependence, which is proved to be valid if no statistically significant difference is revealed between the variance of reproducibility and the least square variance. All three kinds of standard deviation (blank, least-square and general) have been used for calculation of respective detection limits as shown in Table 2. These results confirm that a 6 x 10 mm PZT is the most sensitive option (within a n x 10 mm PZT set tested) in combination with a 10 x 10 x 45 mm rectangular quartz cell with a round corner bottom configuration.

3.2.3 PA cell characteristics for n x 20 mm (height x diameter) PZT set (n = 3, 4, 5, 6, 7, 8 mm)

After a slight modification of PA cell holder in order to accommodate a larger diameter PZT coupled to a 10 x 10 x 45 mm standard cell (Fig. 1a) the similar tests were performed with a 20 mm diameter PZT set. All experimental details described above were used here without any major changes. The corresponding frequency response curves are shown in Fig. 9. One can see much more complex response of PA assembly for this PZT set: no clear maxima is observed for any of the PZT-cell combinations and, that is more important, intensity of PA signal is much weaker in comparison with the previous series, despite of the larger geometrical surface area of

contact between a PZT and the cell.

Apparently, a significant frequency difference between the cell resonance and that of PZT is observed in this case, which does not allow to realize good sensitivity of the entire assembly. As it had become clear from very beginning that this cell–PZT combination is inferior to n x 10 mm PZT diameter set, no full scale calibration experiments were carried out in this case and sensitivity of these assemblies has been roughly estimated using a two point calibration curve (water as a blank solution and a 3.75 x 10^{-4} cm^{-1} solution of Nd(III) at 511.4 nm).

No assessment of detection limit absorptivity was made in view of poor sensitivity of these options and lack of data in calibration experiments (Table 3).

3.2.4 PA cell sensitivity and frequency response for a 20 x 10 x 45 mm rectangular cell in combination with some PZT from n x 10 and n x 20 mm sets

A 20 x 10 x 45 mm rectangular cell has a double optical pathlength in comparison with previously used 10 x 10 x 45 mm one (Fig.1a) and theoretically allows to increase two times the absorbance of a given solution, other conditions being equal. For this reason it seemed interesting to investigate the main photoacoustical characteristics of this cell when coupled to some of available PZT detectors from both sets. One could expect that for this geometry, contrarily to the small cell, a n x 20 mm set might appear to be more effective against the n x 10 mm set. Fig.10 shows frequency responses of this cell assembly for all but 3 x 10 mm PZT from a smaller diameter set and a 6 x 20 mm element which had proved to be most sensitive option in previous experiments with the 10 mm pathlength cell. Again the smaller diameter PZTs proved to be more sensitive with respect 20 mm diameter set but in this case the most sensitive option appeared to be a 8 x 10 transducer rather than a 6 x 10 one as it was found earlier for the 10 x 10 x 45 mm cell.

Although the 6 x 20 element exhibited lower sensitivity than its 6 x 10 analogue, an increase of sensitivity was more than twice in comparison with its response in combination with the 10 mm cell. This indicates that the frequency positions of the cell and the PZT resonances in this case are relatively closer to each other than earlier. Moreover, due to the fact that the 6 x 20 mm PZT – 20 mm cell frequency response is more extended, the intensity of PA signal can be increased in this case by widening of a low–high frequency gate in a band pass filter up to 200 kHz.

Table 4 summarizes the results of calibration experiments for this PA cell assembly. In all cases, if not otherwise indicated, the solution volume was taken 5 ml in order to keep the same height of solution as it was in experiments with the standard 10 mm cell. One can see that longer optical pathlength of PA cell leads indeed to the increase of sensitivity, although in a little bit lesser proportion as compared to the double length of the cell. For explanation of various kinds of

detection limit see comments to Table 2 in section 3.2.2.

Again, as in the case of calibration tests with a 10 x 10 x 45 mm cell, the higher sensitivity does not necessarily correspond to the lower detection limit. This may indicate that not only electromagnetic noise of PZT is the single reason for the fluctiations of PA signal. This question is discussed in more detail in section 3.2.6.

Finally, an additional set of experiments has been carried out on investigation of a PA signal magnitude dependence from volume of solution. Fig.11 shows height profiles of PA signal as a function of distance between laser beam and a bottom of the cell for various amounts of solution. The most intensive PA signal corresponds to solution volume of 3.5 ml, when the laser beam is launched 15 mm above the bottom of the cell (2.5 mm below the lowest point of a concave solution meniscus). This allows to operate with a lesser amount of solution in PA experiment if it is important to reduce solution volume in order to save some valuable or expensive solution constituents used in calibration tests.

An attempt was also made to verify a possibility of further sensitivity enhancement for a 20 mm cell assembly through attachment of not one as usually, but two 10 mm diameter PZT pieces to the bottom of the cell followed by independent amplification of both signals and their mixing using the "A + B" mode of a digital storage oscilliscope. No essential improvement of the PA cell sensitivity was achieved in this case, probably due to less favorable geometrical position of each PZT with respect to an acoustic wave propagation front as compared to the placement of a single PZT in the center of bottom of this cell.

3.2.5 Search for the optimal PZT in combination with a flowthrough 10 x 10 x 45 mm rectangular cell

Preliminary tests of a flowthrough cell (see Fig.1b and section 3.2.1) showed its comparabable sensitivity with a standard cell along with such advantages as lack of necessity to control solution volume and to protect it from dust penetration and evaporation of solvent, although its application requires larger amount of solution due to an additional capacity of tubes in a pumping system. This part describes the results of comparative tests of performance of this cell in combination with various PZT from a n x 10 mm diameter set.

No detailed investigation of frequency response characteristics of this cell was carried out as it was done in above cases (sections 3.2.2 – 3.2.4), because geometrically this cell is similar to a standard 10 x 10 x 45 mm one. Frequency gate positions for each PZT were selected the same as they had been optimized for a standard cell (see section 3.2.2).

The early calibration tests with this cell demonstrated a poor linearity of calibration curves and essential unreproducibility of experimental points from one calibration run to another. In some cases the solution with a higher absorption gave a lower PA signal than a less concentrated solution with lower absorption and vice a verca. The reason for this unreproducibility was

revealed after a careful examination of the sample changing procedure. In order not to spend large amounts of calibration solutions the previously used solution was removed not by diplacement with a new one by a forward stream pumping, but the cell was emptied through the inlet (near to bottom) nozzle using a reverse mode of the peristaltic pump and after that new solution was pumped into the cell while displacing an air space above the rising column of liqiud. It was noticed that this air displacement in many cases was not complete and a small (less than 1 mm) air bubble formed and remained near the output nozzle of the cell.

Further experiments have proved that it was that bubble which strongly affected the propagation of an acoustic wave and caused significant deviation of PA signal from its actual value. The unreproducibility of the signal (for the same solution) from one refilling step to another can be attributed to some difference in bubble size and its location in the upper border of the inner space of the cuvette after each refilling run. As it can be seen from the data of Table 5, this bubble problem caused also significant change in the slope of calibration curve (compare results of two tests with a 4 x 10 mm PZT before and after bubble elimination). From one hand, the bubble presence leads to enhancement of sensitivity of the cell, but a poor reproducibility of results in this case does not allow to consider this enhancement as an advantage of this system.

A 6 x 10 mm PZT element proved again to be the most sensitive option in combination with the flowthrough cell (after an air bubble elimination) as it had been shown earlier for its coupling with a standard cell, however the flowthrough PA cell sensitivity is lower than in the former case.

3.2.6 General analysis of the obtained data (why there is no clear dependence between sensitivity of a PA cell and detection limit absorptivity?)

Comparative investigation of various PZT – cell combinations has given better understanding of some characteristics influencing a PA cell response and its sensitivity. As result of this optimization the most sensitive option comprised by a 20 x 10 x 45 mm cell and a 6 x 10 mm disk shape PZT has been found which possesses by a 5 times higher sensitivity (for solution volume of 3.5 ml) than it was measured earlier for 10 x 10 x 45 mm cell with a 3 x 10 mm PZT (solution volume 2.5 ml) with comparable electric noise levels for both cases. At the same time this advantage has not led to the samefold improvement of the detection limit (hereafter designated as DL) as one could expect theoretically assuming that standard deviation of the experimental points from their least square fitted values (the parameter which is used in a numerator of the formula for calculation of DL) should not be changed appreciably in case of a higher slope of the calibration curve for more sensitive cells. Actually, this is not the case and it is necessary to understand for what reason this deviation grows along with an enhancement of a cell sensitivity.

It is known that electrical noise picked-up by PZT causes significant perturbation of PA signal around its mean value especially for weakly absorbing samples when this noise level can

be comparable in amplitude with PA signal. Averaging of PA signal over a certain number of pulses allows to suppress a noise level and to improve the signal to noise ratio and therefore to reduce a relative standard deviation (RSD) of experimental points used in a calibration experiment. Special experiment was carried out to investigate the reduction of RSD while averaging over the greater number of pulses using water and solution of Nd of two different concentrations. These results are shown on Fig.12, which contains also the noise curve normalized to the RSD value of the water curve for the 256 pulses averaging point. It is clearly seen that a RSD reduction of water signal as a function of averaging conditions does not coincide with the noise reduction trend. This indicates that a PZT noise is not the only source of the PA signal fluctuation.

Among other sources of PA signal fluctuation such factors as the laser beam position stability, the beam profile stability, the pin-hole photodiode time response stability should be mentioned. Moreover, both digital storage oscilloscope and boxcar integrator possess their own uncertainties while measuring the corresponding electrical signals. In case of the boxcar integrator an additional source of uncertainty is connected with a fact that its indicator can display only the integer part of energy signal in mV. This means that, for example, if the measured value of energy signal is indicated as 65 mV (that corresponds to absolute energy level of about 0.8 mJ) its actual value may lie within 64.51 mV – 65.44 mV range if this device can perform round-off procedure or whithin 65.1 – 65.9 mV range if it can't. It is easy to estimate that the relative error of this measurement can reach 0.7% for the first case and 1.3% for the second case. The same consideration may be valid for stability of the boxcar zero line. This error enters further as one of the constituents into the calculated value of normalized PA signal and it can not be eliminated or reduced by any averaging procedure.

As regards the laser beam position stability with respect to PA cell incident point, it has been shown earlier that PA signal is a sensitive function of the beam position and in some cases a 1 mm vertical shift of PA cell against laser beam can cause 15–20% change of PA signal magnitude. This, in turn, means that 0.5% deviation of PA signal can be caused by the as low as 0.025 mm space unstability of laser beam, which is difficult to control experimentally. Laser beam profile variation, caused by unstable operation of the laser dye circulation unit can contribute also to the scattering of PA signal .

Summarizing all abovementioned considerations it is important to stress upon that while the interference of electric noise on PA signal fluctuation can act as the main source of PA signal unstability in case of the weakest absorbances and not sufficient averaging conditions, it has been shown experimentally that relative standard deviation of this signal can not be reduced below 0.4 –0.5% even for very large the signal to noise ratios and good averaging statistics. And as long as the relative standard deviation remains constant, the absolute value of this deviation grows along with absolute value of PA signal, or, in other words, the higher is the sensitivity of PA cell, the

greater is PA signal and, in turn, the greater is absolute deviation of this signal. Therefore, the further improvement of PA spectrometer performance with respect to additional lowering of detection limit of PA cell can be done through the application of a more precise registration electronics and creating more stable conditions for the laser beam generation. In case of strongly absorbing liquid matrixes application of a differential PA cell (consisting of sample and reference cells of the same geometry and with similar PZT responses) can reduce the absolute standard deviation of experimental points from their fitted values in the calibration curve and keep detection limit absorptivity around 1-3 x 10^{-5} cm^{-1}.

3.2.7 More detailed investigation of the PA signal drift and fluctuation in a long term monitoring experiment

A short discussion of the possible sources of data scattering in the PAS experiment was started in the previous section. After that the special long term experiment was conducted, when a large number of data were accumulated during continious registration of PA signal and energy as the time rows. Totally, each experiment consisted of measurement of 200 points of PA signal with the corresponding record of energy; each point, in turn, represented an average value of 512 laser pulses at a 10 Hz repetition rate, so the time for measurement of one point was about one minute and total duration of experiment was more than 3 hours. It was a good chance to understand how the PA signal level and its scattering depends from the corresponding energy parameters and compare reproducibility of results after the signal to energy normalization procedure for a larger number of points.

The first 120 points were recorded using a single portion of solution at state of rest without any manipulations with the cell or other optical components, while the remaining 80 points refer to the case of periodical removal of the "old" (or one may call it "spent") solution from the cell and refilling it with a fresh portion of the same solution. This was repeated after each 10 measuring points, so these data represent 8 blocks, each one consists of 10 readouts. The idea was to check a possible disturbance of PZT characteristics as result of touching the bottom of the cell by a pipette while the sample replacement procedure and to verify whether the processes of a particulate matter settle-down have some influence on PA signal fluctuations.

Two runs of experiments were carried out using highly absorbing (from the photoacoustical point of view) solution of Pr^{3+} at 480 nm and a pure water was taken for the second run as a case of weakly absorbing species at the same wavelength. The results are presented in the Fig. 13, 14. For better understanding of statistical characterictics of PA signal after normalization one more curve is plotted also, which shows its average values calculated for the each 10 points, while the vertical bars illustrate its relative standard deviation expressed in percents. It is clearly seen from both graphs that the primary parameter which can badly influence the fluctuation level of PA signal is the unstability of laser energy. Taking into

account that so great energy fluctuations are observable even after averaging over 512 single shots one can conclude that something is wrong within the laser dye circulating unit. If it is connected with the variation of circulation rate of a dye this can cause also some instability of a laser beam profile which can serve as an additional source of PA signal scattering. The lowest fluctuations of PA signal correspond to the most stable energy output of the dye laser and in this case a larger number of points can be used for statistical averaging of the signal because verification of the hypothesis about uniformity of two (or several) means shows that these blocks of data have statistically the same average values. The sample replacement procedure introduces also some additional scattering of experimental data as one can judge from the greater differences between the average values of PA signal for the last 8 blocks of data in both experiments as compared to the first 12 blocks recorded with a single sample. Probably, the more gentle manipulations with the cell when removing solution and refilling the cell can reduce this source of data scattering down to a single sample level.

3.2.8 Check of PA spectrometer performance in the 459 - 508 nm spectral region (Coumarin-480)

Taking into account that real PAS application in near future will be directed to monitoring of Pu(IV) by its absorption band at 480 nm, which is the most intensive and sharp one among all other absorption peaks of tetravalent plutonium, the PA spectrometer performance has been tested in the blue region of spectrum using a Coumarin-480 laser dye, which, as indicated in the dye laser manual, covers a wavelength range from 459 to 508 nm. Another important peak of interest in this wavelength range is exhibited by the complex of tetravalent technetium with dibutylphosphoric acid (HDBP), with absorption band maximum at 472 nm. This section describes some results of these test experiments performed with aqueous solutions of Pr(III).

(1) PA spectra of Pr(III) aqueous solution

No data on the optimal concentration for Coumarin-480 in the oscillator and amplifier solutions were available from a TDL-580 manual for currently used configuration of laser, that is why the initial concentrations of both solutions were taken the same as it was in case of previously used Coumarin-500 dye and they have been optimized using a stepwise addition of more concentrated dye solution with output energy control after each step. Finally, energy output saturation has been found for the 200 mg/500 ml and 140 mg/500 ml concentrations of the dye in the oscillator and amplifier channels respectively.

After that the dye laser wavelength gain profile was investigated in order to make sure that this feature agrees with the laser manufacturer's data and covers adequately both peaks in the blue region of Pr(III) absorption spectrum. Quite surprisingly, it was found that the actual dye gain profile is essentially narrower from both sides of wavelength scale (470 - 495 nm) as compared

to the Quantel's data (459 – 508 nm).

PA spectra of Pr(III) aqueous solution of two different concentrations were recorded and water absorbance was also investigated for this part of spectrum (see Fig. 15). It is clearly seen that peak positions of Pr(III) absorption bands differ significantly for two concentrations, the lower spectrum looks like artificially shifted to longer wavelengths for about 4 nm. And again, as it had been found earlier for Nd(III) spectrum in the green region (see section 3.2.1, Fig.7), the wavelength distance between two peaks of Pr(III) is shorter for both solutions in comparison with the literature data. The detailed analysis of these wavelength distortions is given in Appendix 2.

(2) Evaluation of detection limit for the 481.3 nm absorption band of Pr(III)

Keeping in mind the laser wavelength uncertainty problems found out in the course of study on Pr(III) PA spectra, the 481.3 nm absorption peak position was carefully examined in a separate wavelength scanning experiment and after the laser emission was tuned to this maximum no other wavelength manipulations were made during calibration tests to avoid any wavelength shift and an accidental change of extinction coefficient.

A number of Pr(III) aqueous solutions were prepared covering absorption range from 5 x 10^{-5} cm^{-1} to 1 x 10^{-3} cm^{-1} and several calibration experiments have been conducted for the selected absorption band using a standard 10 x 10 x 45 mm cell – 6 x 10 mm PZT assembly with solution volume of 2.5 ml under optimized beam incidence conditions. It has been shown that a Coumarin–480 laser emission often caused significant perturbations of PA signal for energies above 0.6 mJ, probably due to excessively high density of laser emission for the narrow beam diameter. In case of Coumarin–500 this effect was observed for energies above 1.5 – 2.0 mJ. Apparently, Coumarin–480 generates more energetic photons in comparison with its longer wavelength analogue and the electrostriction and breakdown phenomena occur at lower laser beam energies than in the former case.

In the course of calibration experiments some registration conditions were varied from one calibration run to another to find conditions for additional reduction of data scattering. In particular, averaging over 512, rather than 256 pulses, has been used, boxcar integrator has been switched from exponential mode to averaging mode and the energy signal was amplified 10 times before its feeding to the boxcar in order to reduce a round–off error of this device. All these measures allowed to lower the detection limit of PA spectrometer from 3.3 x 10^{-5} cm^{-1} (first experiment) to 1.2 x 10^{-5} cm^{-1} (final run) for the 481.3 nm absorbtion band of Pr(III), despite of artificially reduced laser beam energy (< 0.6 mJ). Calibration curves showed a good linearity as one can judge from comparison of general and least square deviations of experimental points. Detection limit calculated through a PA signal deviation of blank solution (water) gave in some cases even n x 10^{-6} cm^{-1} values (n=6–8).

3.3 PAS application to detection of simulated Pu(IV), Pu(III) and Pu(VI) species in U(VI) containing solutions

As it has been already mentioned in the experimental part of this report (see section 2.3), a number of non radioactive substituents were used to imitate some absorption band maxima of Pu(III), Pu(IV) and Pu(VI) in aqueous solution (see Fig.16 illustrating absorption spectra of Pu in different oxidation states [7]).

3.3.1 Background absorption characteristics of U(VI) solutions in aqueous phase and in 30% TBP solution in n-dodecane in the blue-green range of spectrum

A $UO_2(NO_3)_2$ solution in 3N HNO_3 (10g/l of uranium) was prepared for investigation of its photoacoustic properties, because in many cases of future PAS application to monitoring of the actinide and/or fission product species in nuclear fuel reprocessing solutions uranyl nitrate may often occur as a background component, probably interfering with a detected species. Despite of its relatively low molar absorption coefficient its concentration may be high that can cause significant increase of background absorption well above the water absorption level even in the wavelength region not related to its main peak at 415 nm. Two Coumarin dyes were used to cover the spectral region from 464 nm to 533 nm. The PA spectra of uranyl nitrate aqueous solution are presented separately for C-480 and C-500 in the Figs. 17 and 18 respectively. Each figure contains also the spectrum of the TBP extracted uranyl species in organic phase (30% TBP in n-dodecane). This is important also for future PAS application when the need will arise to monitor some extracted species of interest in organic phase.

As it follows from the Fig. 17 , if one would try to characterize the absorbance of uranyl species in aqueous phase as very high (in photoacoustical scale), he must then use the term "enormous" for its spectrum in organic phase. Obviously, a long wavelength shift of the absorption spectrum of UO_2-TBP extracted species takes place in organic phase which causes such an increase of absorptivity and poses serious doubts in applicability of PAS detection of minor components in the uranium containing organic systems with TBP in this spectral range for uranium concentration higher than 10 g/l. In the C-500 generation range (Fig. 18) the absorption in organic phase drops rapidly toward the green part of spectrum and after a small peak around 508 nm it closely approaches the absorption curve of uranyl nitrate in aqueous phase. Comparing with PA signal from water near 520-530 nm range one can see that UO_2^{2+} aqueous solution exhibits 2 - 2.5 times higher absorbances only.

It is interesting to observe that starting after 512 nm the absorption of pure extractant (30% solution of TBP in dodecane) goes higher than that of extracted uranium species in the same medium (Fig. 18). The explanation may consist in the fact that as a result of contact with aqueous phase TBP interacts with water forming some hydrated species which can have lower

absorptivity in this spectral range compared with anhydrous solution of TBP.

3.3.2 Problem of a positive drift of PA signal in the strongly absorbing part of uranyl spectrum in organic phase

In the process of investigation of PAS spectrum of the uranyl–TBP complex in organic phase a need arose to accumulate more representative body of data on the level of PAS signal at 480 nm. When this experiment was started it has become clear that there was no normally occuring statistical fluctuation of the signal around its mean value, but the signal exhibited a positive drift in time from one point to another (see Fig.19 for illustration). This drift continued for more than 12 minutes of observation and caused the increase of signal on about 30% above the initial value. After that a 10% optical filter was inserted on the way of laser beam to the cell and the measurements were continued. Immediately after the beam attenuation the normalized PA signal started to drop monotoneously and after 25 minutes of observation its value reached saturation at the level 10% lower than the very first value of signal when the full energy was applied to solution. Apparently, the nature of this effect lies in the process of the heat release as result of the light energy conversion into the thermal one which causes the heating of solution to much greater extent than it happens in weakly absorbing liquids. This, in turn, results in the change of physical properties of the medium and, in particular, a coefficient of isobaric compressibility of TBP–dodecane solution, which is, likewise for the aqueous solution case, can be one of the major temperature influenced parameters determining the level of PA signal in organic phase.

3.3.3 Calibration experiment for estimation of detection limit for Pu(IV) species at 480 nm using Pr(III) peak as imitation of Pu(IV) absorption

The most intensive absorption peak of Pu(IV) at 480 nm (= 69 l/mol cm^{-1}) was selected initially for examination of PAS capabilities at this wavelength. Significant point scattering around their least square fitted values has resulted in more than one order loss of detection limit. The main reason for this result is high background absorption of uranyl ions at the selected wavelength and this is consistent with the abovementioned consideration about impossibility to improve the relative error of PA signal below 0.4–0.5% under existing experimental conditions.

3.3.4 Calibration experiment for Pu(IV) species at 550 nm imitated by a Cr(III) absorption band

Although Coumarin–500 is reported to have a long wavelength border of generation of about 559 nm, its actual generation threshold does not exceed 534 nm. One of the possible

reasons for this discrepancy may be related to not enough purity of methanol used for preparation of the dye solution. The laser manufacturer warns that only high quality methanol must be used for this procedure to ensure the laser dye generation in the widest possible range. F-548 dye pumped by the second harmonics of Nd(YAG) laser has been used to provide generation at 550 nm. Its oscillator and amplifier concentrations were optimized experimentally and after adjustment of optical parts of TDL-500 laser beam energy at this wavelength has grown up to 10 mJ.

As it was already mentioned, aqueous solution of Cr(III) ions was used for imitation of Pu(IV) absorption band at 550 nm. Significant decrease of background absorption level of uranyl species and more favorable laser beam profile generated by the new dye were the decisive factors in attaining the lowest detection limit absorptivity (0.98×10^{-5} cm^{-1}) for the case of direct laser beam introduction into the cell.

Optical fiber launching arrangement was tested then at the same wavelength. This experiment was conducted without beam collimation procedure (see section 3.3.7 for more detailed description of this approach). The detection limit absorptivity attained (1.72×10^{-5} cm^{-1}) is the best one ever obtained in the course of this research project for the experiments with optical fibers.

3.3.5 Calibration experiment for detection of Pu(III) species at 562 nm imitated by a Cr(III) absorption band

The same dye was used for laser light generation at 562 nm and the same absorption band of Cr(III) was applied for simulation of Pu(III) absorption at the wavelength selected. Although detection limit absorptivities are a little higher than in previous case for Pu(IV), the more intensive absorption band of Pu(III) (= 38 l/mol cm^{-1}) allows its reliable detection at a low micromolar level.

3.3.6 PAS detection of Pu(VI) species by its peak at 525 nm imitated by Nd(III).

The possibility of Pu(VI) detection was examined using absorption band of Nd(III) at 522 nm for imitation of plutonium peak at 525 nm (= 13 l/mol cm^{-1}). The detection limit absorptivity was found to be 1.6×10^{-5} cm^{-1}, that corresponds to 1.23×10^{-6} M concentration of Pu(VI). No optical fiber transmission arrangement was tested in this case.

Table 6 summarizes the results of all PAS experiments on detection of various Pu species in the uranium containing solution.

3.3.7 Simplified optical fiber launching arrangement and possibility of PAS detection for noncollimated laser beam propagation through a rectangular PA cell

Usually application of optical fibers for laser light transmission from laser to a PA cell requires installation of some additional optical components at the output end of fiber to reduce a beam divergence and to fit its propagation profile to the cell geometry. Earlier, following the recommendations of Silva and co-authors [6], we have shown that a microscope objective can be effectively used for this purpose which made it possible to improve the linearity of calibration curve and to reach lower detection limits both for cylindrical long path cell and especially for a rectangular type cuvette cell. Application of an objective inevitably causes 15-20% drop of the light intensity due to Freshnel losses on its lens surfaces and a care must be taken to avoid an optical burn-up of its lens coating when applying a higher amount of laser energy. The objective must be attached to a X-Y-Z translation stage for the fine adjustment of its position with respect to output end of fiber.

The fiber used in our experiments has a relatively large core diameter (1.2 mm) allowing not to pay so much attention to a precise focusing of the laser beam at its input head and, moreover, it was found that a beam divergence is not so large in this case as compared to the light guides with a thinner core diameter. Taking into account all these considerations we tried to study a PA cell response to the incident laser beam directly after its output from the fiber without using any objectives or other optical parts for the beam collimation. The cuvette cell was placed 4 mm after the output end of fiber where the beam diameter increased approximately to 2 mm. As result of beam divergence its light spot diameter on the rear wall of the cell was 3.0 - 3.2 mm. Our main concern was to avoid hitting the side walls of the cell and upper interface of solution by the ring-type light zone which is clearly seen in the light cross section spot structure as a peripheral ring formation spatially separated from the main light spot (see Fig.3 for illustration of this feature). Its rapid widening requires a special care for the cell adjustment to avoid light scattering phenomena inside the cell. It was informative to judge about the efficiency of this adjustment by observing an oscilloscope picture of PA signal which showed a large increase of the initial part of the signal (2-3 mcs after the trigger pulse) in case of improper beam positioning relative to the cell borders, when the reflected or scattered light lit the PZT. Finally, though no complete suppression of the PZT response to the scattered and reflected light was achieved, the most appropriate cell position was found corresponding to minimum disturbance of the pure compression wave structure of PA signal.

One more innovation was tested in the course of this experiment: laser beam exiting the cell and leaving then a noise shielding container was not focused onto the energy measuring photodiode, but directed on its surface as result of its natural propagation . The size of a light spot reaching the photodiode was about 20 mm in diameter, so only a small part of whole energy was registered by the diode. Before feeding this signal to a boxcar integrator the signal was amplified

20 times in order to provide a three digits readout value (hundreds of millivolts) in the energy channel and to reduce a round-off error of the integrator. This arrangement was tested several times in the course of calibration experiments with the Pu(IV) and Pu(III) nonradioactive substituents in the uranyl containing solutions at 550 nm and 562 nm respectively. A 4 mm distance between the output head of fiber and the front wall of the cell has proved to be a good compromise between a PA signal perturbation due to excessive density of laser energy for the shorter distance and a light scattering problems of laser beam inside the cell for a longer distance. Both calibration curves show good linearity and the corresponding detection limits are comparable with the previously evaluated values for the case of direct beam introduction.

Therefore, the simplified optical fiber launching arrangement tested in this work has proved to be not less effective in comparison with the the beam collimating arragement and it allows to perform a PA detection of weakly absorbing species with detection limits about 1.5 – 2.5 x 10^{-5} cm^{-1}. It is difficult to say why Silva et al. [6] did not consider such a simple and effective possibility of PAS arrangement. Probably, the optical fiber they used in their work had not so favorable beam divergence profile due to a much thinner core diameter.

4. CONCLUSION

The main results of the research project can be summarized as follows:

1) A cylindrical flowthrough PA cell with the optical pathlength of 100 mm can be effectively used for monitoring of weakly absorbing species only in case of a direct laser beam introduction into the cell. It is not suitable for optical fiber launching arrangement due to impossibility to provide a proper beam collimation along the entire optical distance even using a microscope objective that causes one order loss of detection limit absorptivity of the cell.

2) Newly tested cuvette type spectrophotometric cells in combination with a disk type PZT exhibit high sensitivity and good linearity of the calibration curve both for direct laser beam introduction and for light transmission through an optical fiber due to negligible contribution of scattered and reflected light to PZT response in case of collimated laser beam propagation. This results in lowering of detection limit down to (1–2.5) x 10^{-5} cm^{-1}, which allows to perform a reliable detection of many species of actinide elements at micromolar concentration level in the water like absorbing matrixes.

3) Results of PAS application to detection of simulated Pu(III), Pu(IV) and Pu(VI) species in uranium containing solution using the newly designed cells have shown that proper selection of

20 times in order to provide a three digits readout value (hundreds of millivolts) in the energy channel and to reduce a round-off error of the integrator. This arrangement was tested several times in the course of calibration experiments with the Pu(IV) and Pu(III) nonradioactive substituents in the uranyl containing solutions at 550 nm and 562 nm respectively. A 4 mm distance between the output head of fiber and the front wall of the cell has proved to be a good compromise between a PA signal perturbation due to excessive density of laser energy for the shorter distance and a light scattering problems of laser beam inside the cell for a longer distance. Both calibration curves show good linearity and the corresponding detection limits are comparable with the previously evaluated values for the case of direct beam introduction.

Therefore, the simplified optical fiber launching arrangement tested in this work has proved to be not less effective in comparison with the the beam collimating arragement and it allows to perform a PA detection of weakly absorbing species with detection limits about 1.5 – 2.5 x 10^{-5} cm^{-1}. It is difficult to say why Silva et al. [6] did not consider such a simple and effective possibility of PAS arrangement. Probably, the optical fiber they used in their work had not so favorable beam divergence profile due to a much thinner core diameter.

4. CONCLUSION

The main results of the research project can be summarized as follows:

1) A cylindrical flowthrough PA cell with the optical pathlength of 100 mm can be effectively used for monitoring of weakly absorbing species only in case of a direct laser beam introduction into the cell. It is not suitable for optical fiber launching arrangement due to impossibility to provide a proper beam collimation along the entire optical distance even using a microscope objective that causes one order loss of detection limit absorptivity of the cell.

2) Newly tested cuvette type spectrophotometric cells in combination with a disk type PZT exhibit high sensitivity and good linearity of the calibration curve both for direct laser beam introduction and for light transmission through an optical fiber due to negligible contribution of scattered and reflected light to PZT response in case of collimated laser beam propagation. This results in lowering of detection limit down to (1–2.5) x 10^{-5} cm^{-1}, which allows to perform a reliable detection of many species of actinide elements at micromolar concentration level in the water like absorbing matrixes.

3) Results of PAS application to detection of simulated Pu(III), Pu(IV) and Pu(VI) species in uranium containing solution using the newly designed cells have shown that proper selection of

absorption band of the detected chemical form of plutonium to avoid high background absorption level of uranyl ion in the blue part of spectrum makes it possible to keep detection limit absorptivity whithin the 1.5 – 2.5 x 10^{-5} cm^{-1} range. It has been shown also that a new configuration of PA cell can be successfully used in optical fiber launching arrangement for the case of noncollimated laser beam propagation. This allows to simplify significantly the experimental setup by excluding several optical components and to reduce a number of adjustment procedures of PA spectrometer. The detection limit in this arrangement has been found to be 9 x 10^{-7} mol/l for Pu(IV) at 550 nm and 6.1 x 10^{-7} mol/l for Pu(III) at 562 nm, both values refer to the presence of 10 g/l of uranium(VI) in solution.

Acknowledgements

The authors wish to express their gratitude to Dr. I.Kobayashi for his efforts on getting the JAERI Research Fellow position for Dr. S.I.Sinkov allowing him to participate in this research project.

Dr. Z.Yoshida's critical reading of the manuscript and his many valuable suggestions on modification of its content and structure are also gratefully acknowledged.

absorption band of the detected chemical form of plutonium to avoid high background absorption level of uranyl ion in the blue part of spectrum makes it possible to keep detection limit absorptivity whithin the 1.5 – 2.5 x 10^{-5} cm^{-1} range. It has been shown also that a new configuration of PA cell can be successfully used in optical fiber launching arrangement for the case of noncollimated laser beam propagation. This allows to simplify significantly the experimental setup by excluding several optical components and to reduce a number of adjustment procedures of PA spectrometer. The detection limit in this arrangement has been found to be 9 x 10^{-7} mol/l for Pu(IV) at 550 nm and 6.1 x 10^{-7} mol/l for Pu(III) at 562 nm, both values refer to the presence of 10 g/l of uranium(VI) in solution.

Acknowledgements

The authors wish to express their gratitude to Dr. I.Kobayashi for his efforts on getting the JAERI Research Fellow position for Dr. S.I.Sinkov allowing him to participate in this research project.

Dr. Z.Yoshida's critical reading of the manuscript and his many valuable suggestions on modification of its content and structure are also gratefully acknowledged.

References.

1) Klenze R. and Kim J.I. A direct speciation of transuranium elements in natural aquatic systems by laser-induced photoacoustic spectroscopy: Radiochim. Acta 44/45, 77 (1988)

2) Beitz J., Doxtader M.M., Maroni V.A., Okajima S. and Reed D.T. High Sensitivity photo-acoustic spectrometer for variable temperature solution studies: Rev.Sci.Instrum, 61, 1395 (1990)

3) Torres R., Palmer C.E., Baisden P.A., Russo R.E. and Silva R.J. Comparison of photoacoustic spectroscopy, conventional absorption spectroscopy and potentiometry as probes of lanthanide speciation: Anal. Chem. 62, 298 (1990)

4) Kihara T., Fujine S., Maeda M., Matsui T., Fukasawa T., Sakagami M., Ikeda T., Kitamori T. Development of a laser induced photoacoustic spectroscopy system for analytical technique of Np ion in the PUREX process. JAERI-M 91-142 (1991)

5) Kihara T., Fukasawa T., Fujine S., Maeda M., IkedaT., Kawamura F. Development of sensitive analytical technique by laser induced photoacoustic spectroscopy. JAERI-M 93-234 (1993)

6) Russo R.E., Rojas D., Robouch P., and Silva R.J.: Remote photoacoustic measurements in aqueous solutions using an optical fiber. Rev.Sci.Instrum. 61, 3729 (1990)

7) Gangwer T. Photochemistry relevant to nuclear waste separations. A feasibility study. BNL 50715. Brookhaven National Laboratory, 1977, 138 p.

Table 1 Correction coefficients for calculation of exact concentration value of absorbing solute during a single sample calibration experiment (amount allignment of solution in the cell is taken to be equal 2.500 mcl)

Number of the concentration point	Portion of stock solution, v, mcl	Simplified concentration coefficient	Real concentration coefficient	Column4/column3 ratio
1	0 0	---------- ----------	--------- ---------	-------- --------
2	20 100	1 1	1 1	1 1
3	40 200	2 2	1.992 1.96	0.996 0.98
4	60 300	3 3	2.976 2.882	0.992 0.961
5	80 400	4 4	3.952 3.766	0.988 0.942
6	100 500	5 5	4.921 4.616	0.984 0.923
7	120 600	6 6	5.881 5.431	0.980 0.905
8	140 700	7 7	6.834 6.214	0.976 0.888

(*) See Appendix 1 for more detailed description of a single sample calibration experiment.

Table 2 Characteristics of PA cell assemblies based on a standard spectrophotometric cell (45×10×10 mm) in combination with various disk type PZT for 10 mm diameter set.

PZT dimensions, thickness x diameter, mm	Optimum frequency range, KHz	Sensitivity, $1/cm^{-1}$, expressed as a slope of calibration curve	Det. limit absorptivity by dispersion of blank solution, cm^{-1}	Det. limit absorptivity by least square dispersion, cm^{-1}	Det. limit absorptivity by general dispersion, cm^{-1}	Noise level, mV for averaging by 256 pulses
3 x 10	160 - 260	2570	2.4×10^{-5}	2.6×10^{-5}	2.4×10^{-5}	10.3
4 x 10	150 - 250	3470	2.6×10^{-5}	2.0×10^{-5}	3.8×10^{-5}	11.7
5 x 10	150 - 250	2550	3.3×10^{-5}	6.6×10^{-5}	4.3×10^{-5}	12.9
6 x 10	140 - 240	4620	2.3×10^{-5}	1.5×10^{-5}	2.1×10^{-5}	16.1
7 x 10	130 - 230	4520	2.1×10^{-5}	1.6×10^{-5}	2.5×10^{-5}	15.6
8 x 10	120 - 220	4540	1.3×10^{-5}	2.3×10^{-5}	2.3×10^{-5}	15.2

Table 3 Characteristics of PA cell assemblies based on a standard spectrophotometric cell (45×10×10 mm) in combination with various disk type PZT for 20 mm diameter set.

PZT dimensions, thickness x diameter, mm	Optimum frequency range, KHz	Sensitivity, $1/cm^{-1}$, expressed as a slope of calibration curve (*)	Noise level, mV for averaging by 256 pulses
3 x 20	80 - 180	430	15.5
4 x 20	180 - 280	1230	16.5
5 x 20	130 - 230	530	14.7
6 x 20	100 - 200	1830	16.0
7 x 20	200 - 300	570	17.5
8 x 20	50 - 150 (230 - 330)	1340	16.5

(*) Rough estimates based on the two points concentrational dependence

Table 4 Characteristics of PA cell assemblies based on a standard spectrophotometric cell (45×10×20 mm) in combination with various disk type PZT for 10 mm diameter set.

PZT dimensions, thickness x diameter, mm	Optimum frequency range, KHz	Sensitivity, $1/cm^{-1}$, expressed as a slope of calibration curve	Det. limit absorptivity by dispersion of blank solution, cm^{-1}	Det. limit absorptivity by least square dispersion, cm^{-1}	Det. limit absorptivity by general dispersion, cm^{-1}	Noise level, mV for averaging by 256 pulses
5 x 10	150 - 250	4450	8.8×10^{-6}	1.0×10^{-5}	1.9×10^{-5}	12.0
6 x 10	120 - 220	6980	1.0×10^{-5}	1.2×10^{-5}	1.3×10^{-5}	11.7
7 x 10	100 - 200	7480	1.0×10^{-5}	1.6×10^{-5}	1.9×10^{-5}	11.3
8 x 10	100 - 200	7910	0.6×10^{-5}	1.7×10^{-5}	1.7×10^{-5}	13.3
8 x 10 (*)	100 - 200	11010	0.9×10^{-5}	1.7×10^{-5}	1.6×10^{-5}	13.3
6 x 20	80 - 280	4930	1.3×10^{-5}	2.7×10^{-5}	2.2×10^{-5}	10.0

(*) Solution volume is 3.5 ml.

Table 5 Characteristics of PA cell assemblies based on a flowthrough spectrophotometric cell (45×10×10 mm) in combination with various disk type PZT for 10 mm diameter set.

PZT dimensions, thickness x diameter, mm	Optimum frequency range, KHz	Sensitivity, $1/cm^{-1}$, expressed as a slope of calibration curve	Det. limit absorptivity by dispersion of blank solution, cm^{-1}	Det. limit absorptivity by least square dispersion, cm^{-1}	Det. limit absorptivity by general dispersion, cm^{-1}
3 x 10	160 - 260	2390	1.7×10^{-5}	2.0×10^{-5}	3.1×10^{-5}
4 x 10 (*)	150 - 250	4240	2.0×10^{-5}	2.8×10^{-5}	1.7×10^{-5}
4 x 10	150 - 250	2510	2.3×10^{-5}	2.7×10^{-5}	2.8×10^{-5}
5 x 10 (*)	150 - 250	3740	1.8×10^{-5}	1.8×10^{-5}	4.0×10^{-5}
6 x 10	140 - 240	3210	0.9×10^{-5}	2.0×10^{-5}	2.2×10^{-5}
7 x 10 (*)	130 - 230	3550	2.5×10^{-5}	1.0×10^{-5}	2.8×10^{-5}

(*) Small air bubble was noticed in the top part of the cell, which was formed every time after replacement of calibration solutions due to poor wettability of inner surface near the output nozzle.

Table 6 Evaluation of PAS capabilities for detection of various oxidation states of plutonium using simulated Pu species in uranium(VI) containing solution*.

Reagent used for imitation of the corresponding absorption band of Pu and absorption band maximum positions, nm	Molar absorption coefficient of Pu absorption band, l/mol cm^{-1}	Direct laser beam introduction		Optical fiber launching arrangement	
		Detection limit absorptivity, 1/cm	Detection limit concentration, M	Detection limit absorptivity, 1/cm	Detection limit concentration, M
Cr(III) (Pu(III)) 562	38	1.70×10^{-5}	4.5×10^{-7}	2.33×10^{-5}	6.1×10^{-7}
Pr(III) (Pu(IV)) 480	69	4.22×10^{-4}	6.1×10^{-6}	----------	
Cr(III) (Pu(IV)) 550	19	0.98×10^{-5}	5.2×10^{-7}	1.72×10^{-5}	9.0×10^{-7}
Nd(III) (Pu(VI)) 525	13	1.60×10^{-5}	1.2×10^{-6}	----------	

*Remote calibration experiments were performed under condition of noncollimated laser beam propagation after exiting the optical fiber (without using a microscope objective lens)

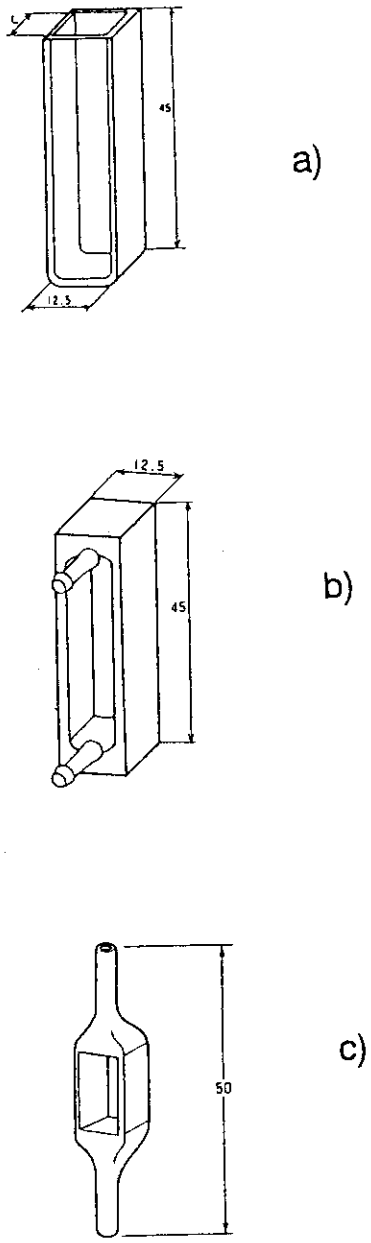

Fig. 1 Cuvette type cells for development of a short optical pathlength cell
a) S10U type standard cell with round corner bottom
b) FL30 type flow through cell
c) FL80 type flow cell

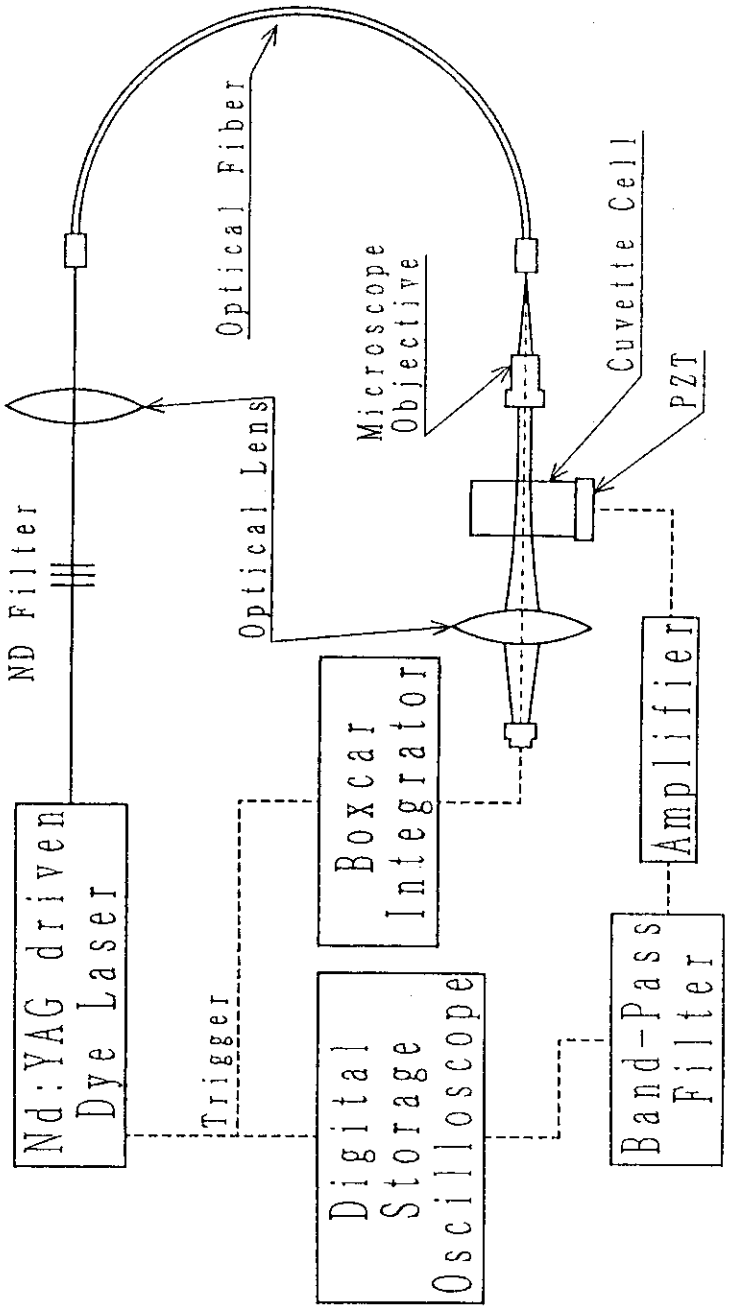

Fig. 2 Experimental setup of Optical Fiber PAS

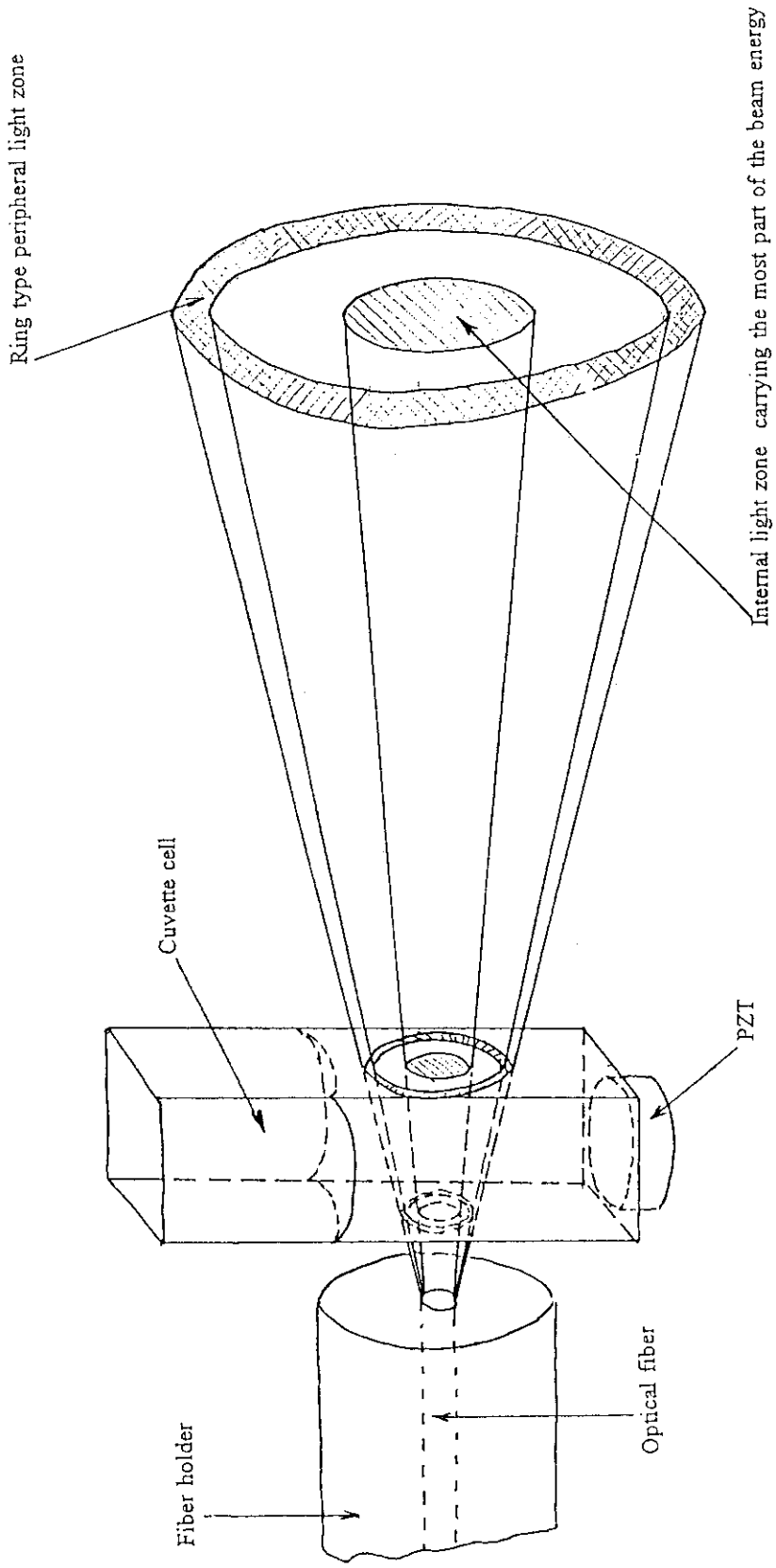

Fig. 3 Illustration of noncollimated beam propagation through the rectangular cuvette cell

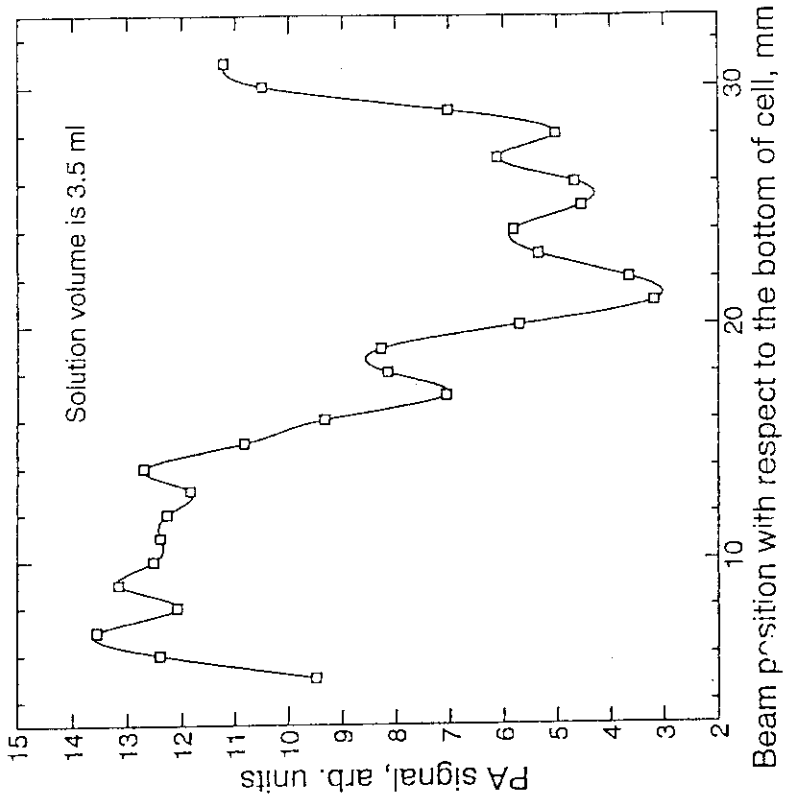

Fig. 5 PA signal as a function of distance between laser beam and PZT (S10U type standard cell)

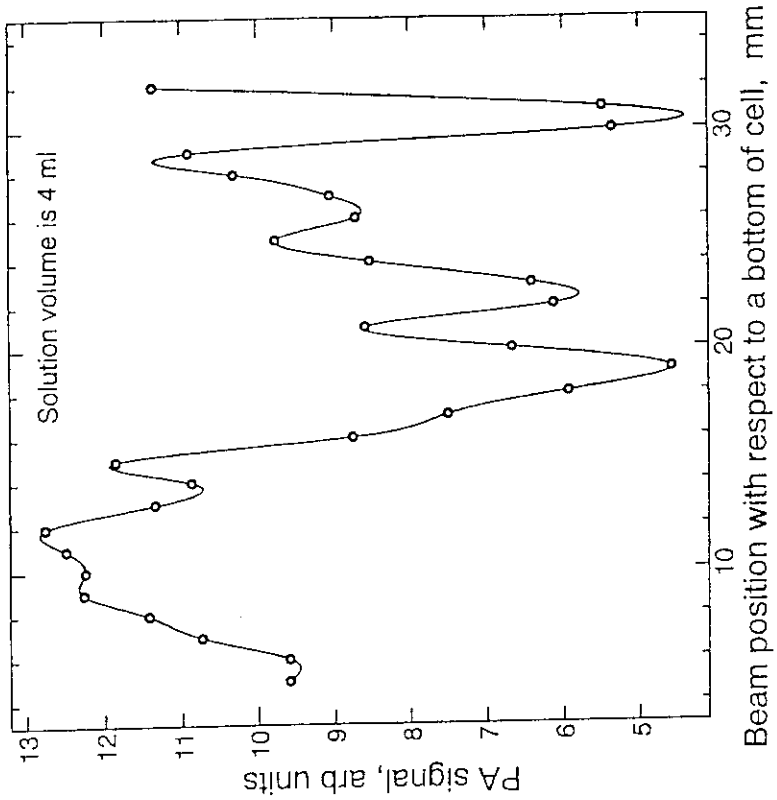

Fig. 4 PA signal as a function of distance between laser beam and PZT (S10U type standard cell)

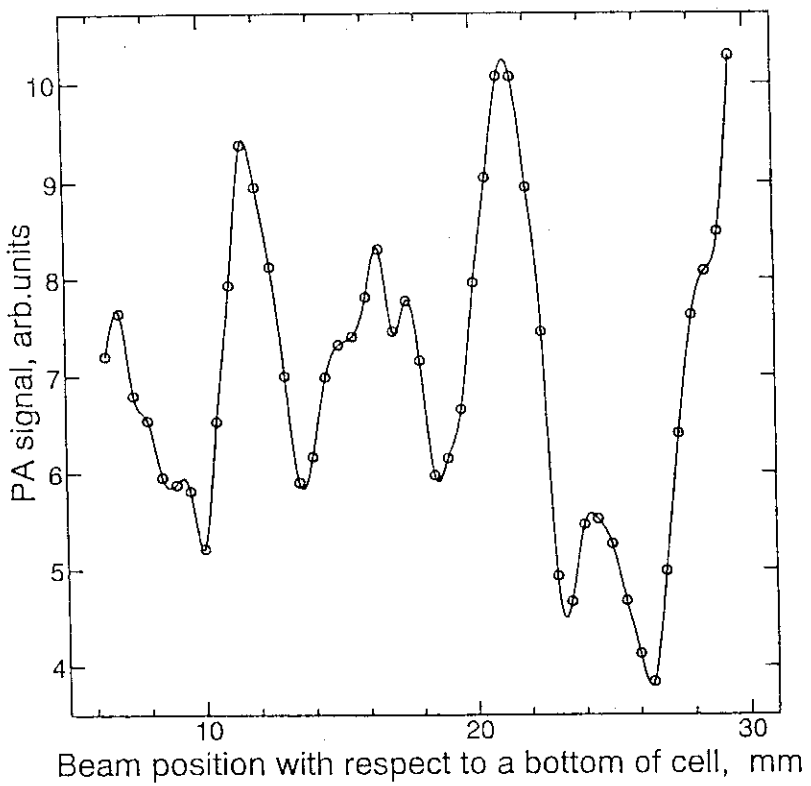

Fig. 6 PA signal as a function of distance between laser beam and PZT (FL30 flow through cell)

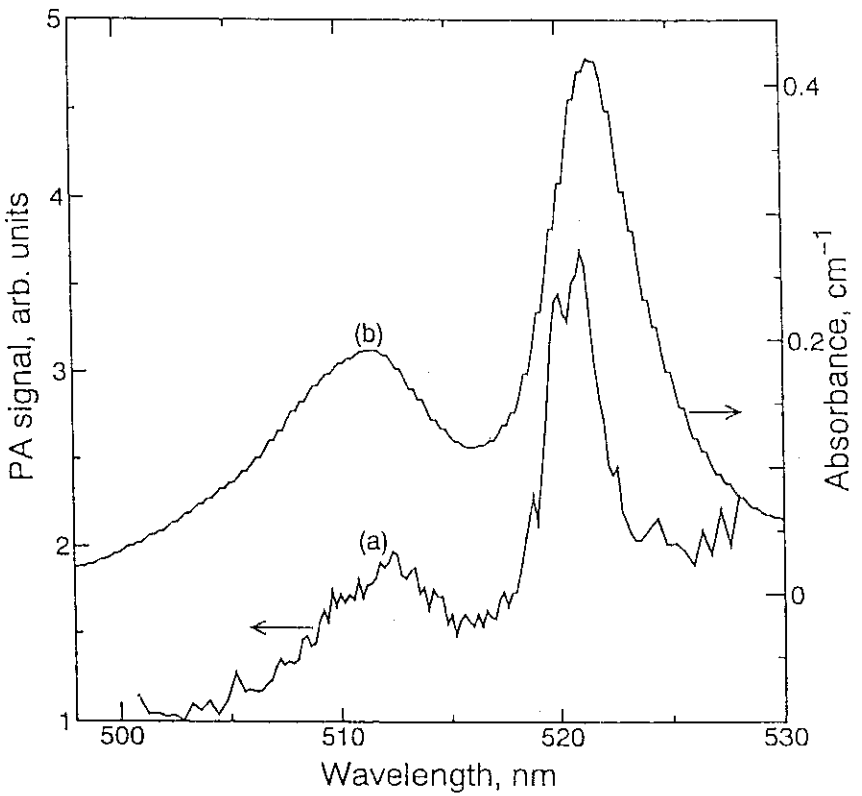

Fig. 7 Comparison of spectra of Nd(Ⅲ)
a) Photoacoustic spectrum (2.1×10^{-4}M)
b) Absorption spectrum (0.105 M)

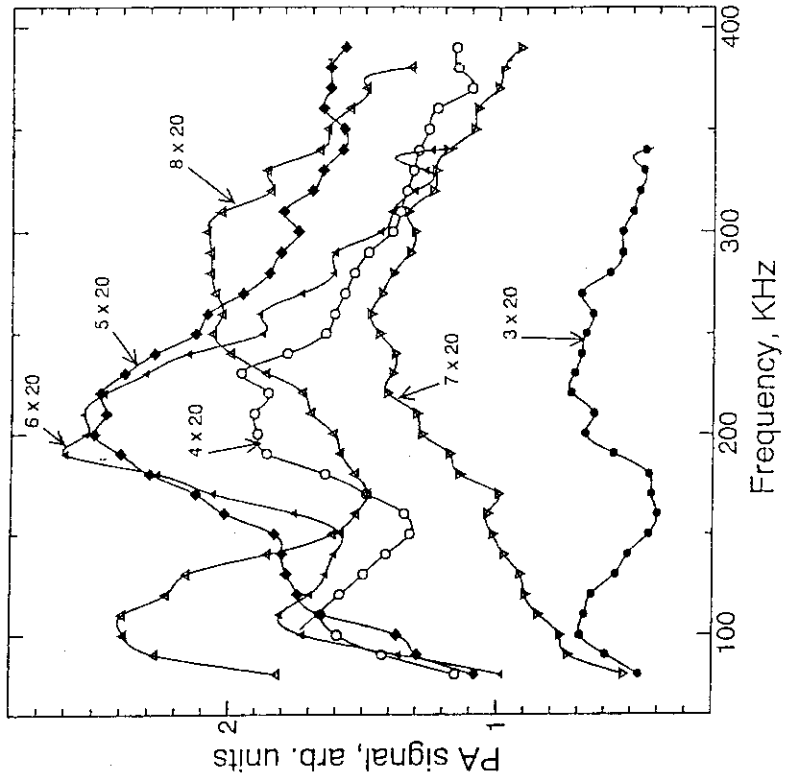

Fig. 9 Frequency response of a standard PA cell with a 20 mm diameter PZT set

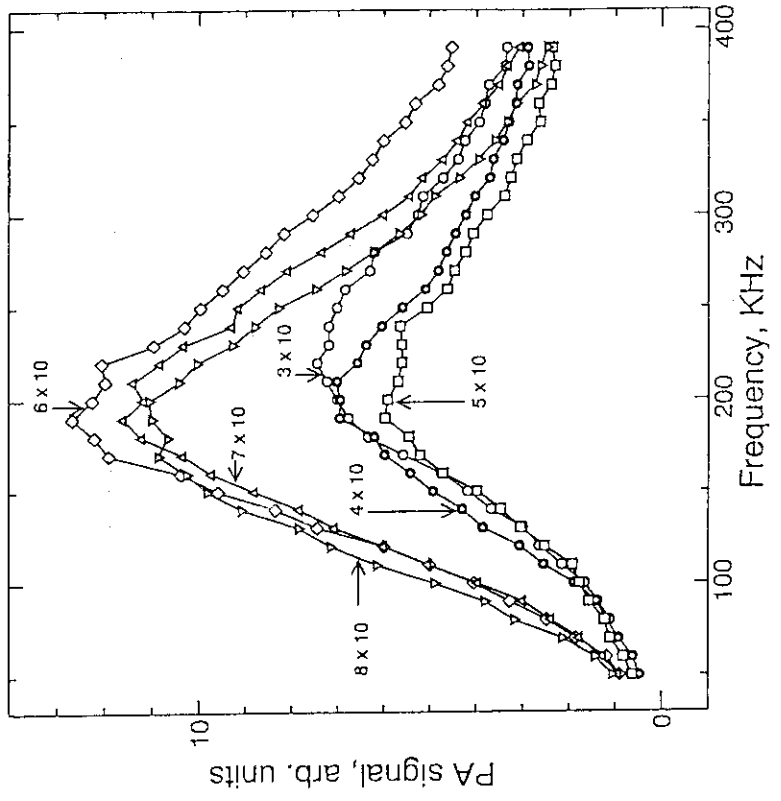

Fig. 8 Frequency response of standard PA cell with a 10 mm diameter PZT set

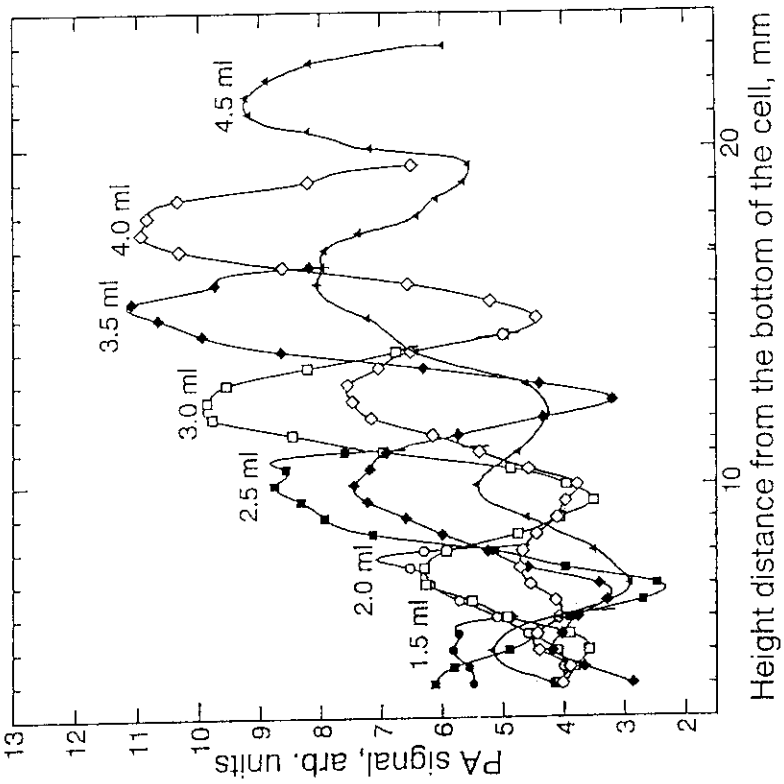

Fig. 11 Height profiles of PA signal for various amounts of solution (a 20×10×45 mm PA cell)

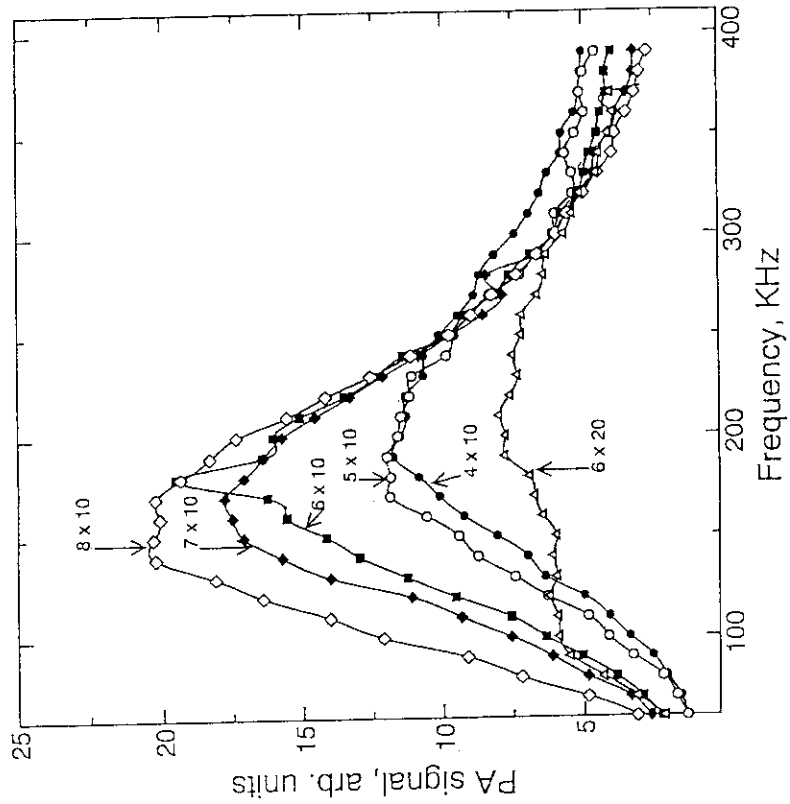

Fig. 10 Frequency response of a 20×10×45 mm PA cell with various PZT

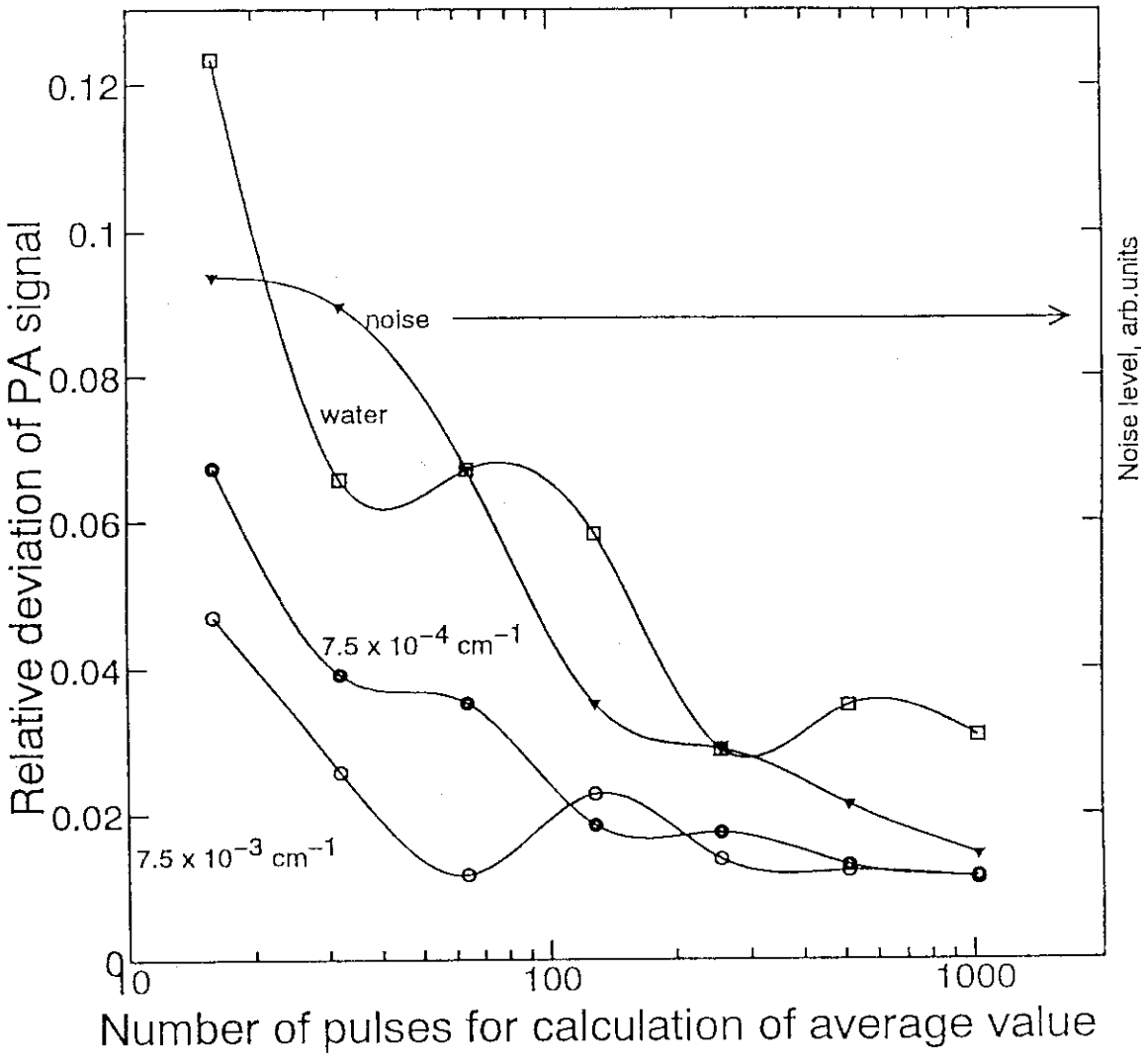

Fig. 12 Relative deviation of PA signal as a function of a number of pulses used for averaging

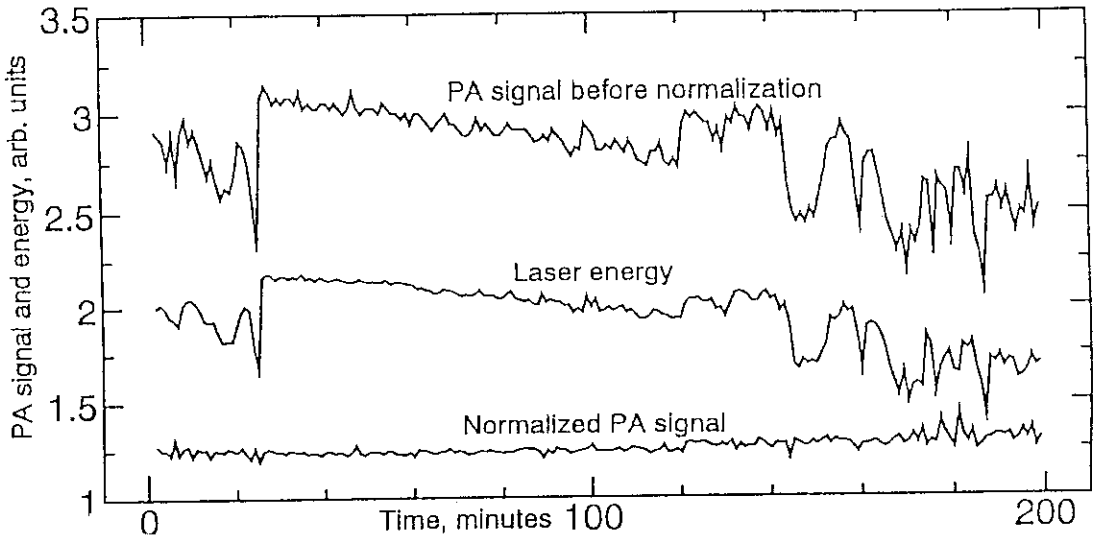

Fig. 13a Illustration of PA spectrometer performance for strongly absorbing species (S/N ratio is 120)

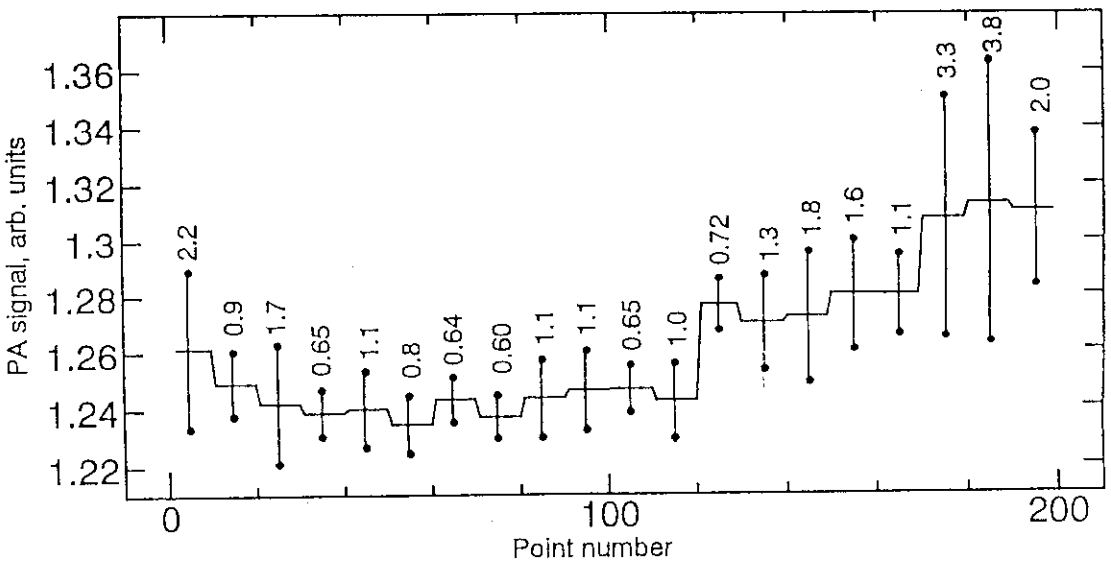

Fig. 13b Averaged values of PA signal for the group of 10 points from the upper picture (vertical bars represent RSD, %)

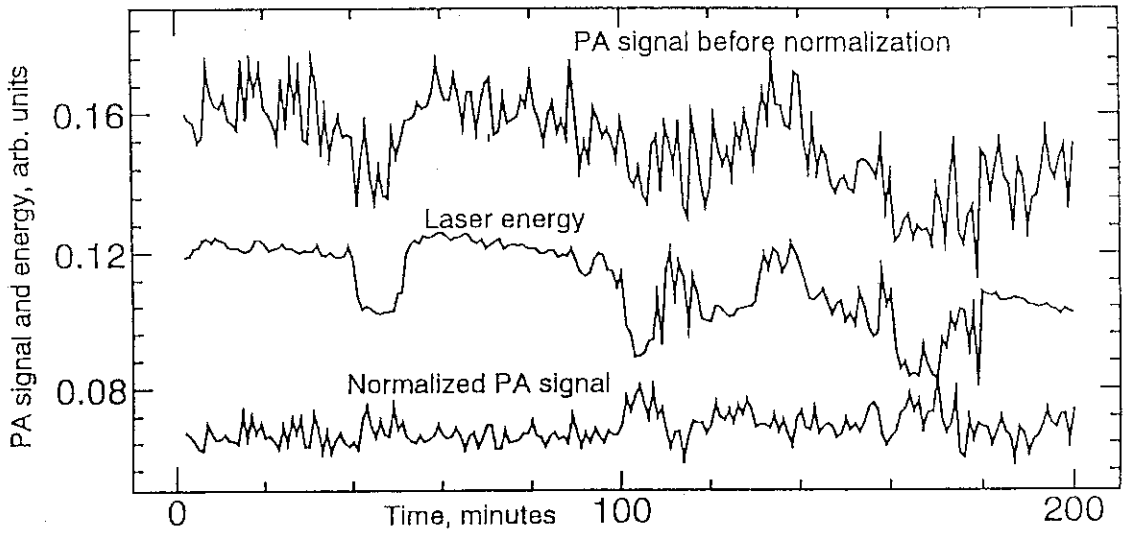

Fig. 14a Illustration of PA spectrometer performance for weakly absorbing species (S/N ratio is 4)

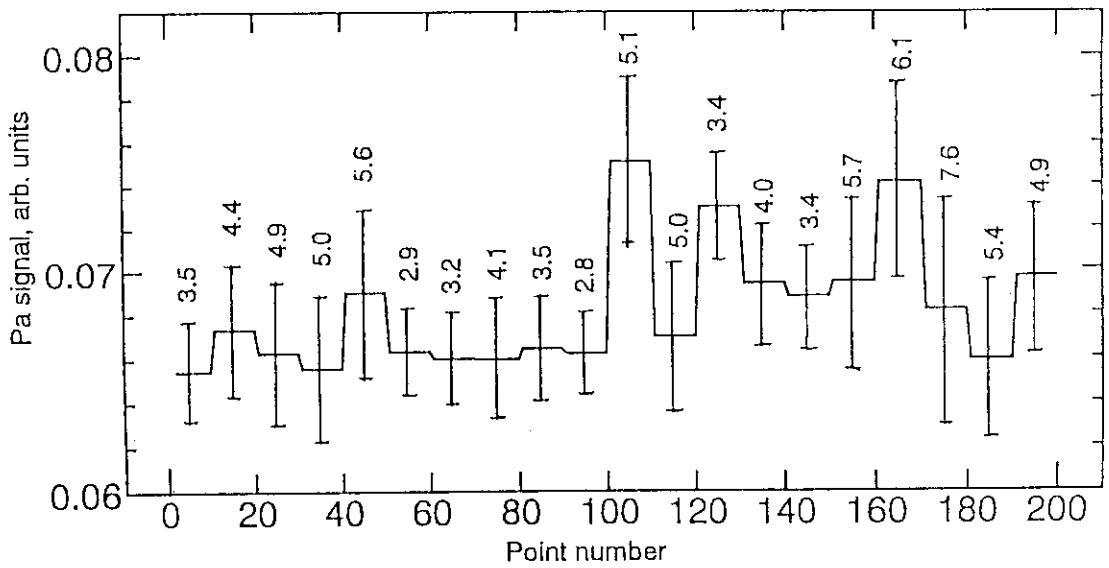

Fig. 14b Averaged values of PA signal for the group of 10 points from the upper picture (vertical bars represent RSD, %)

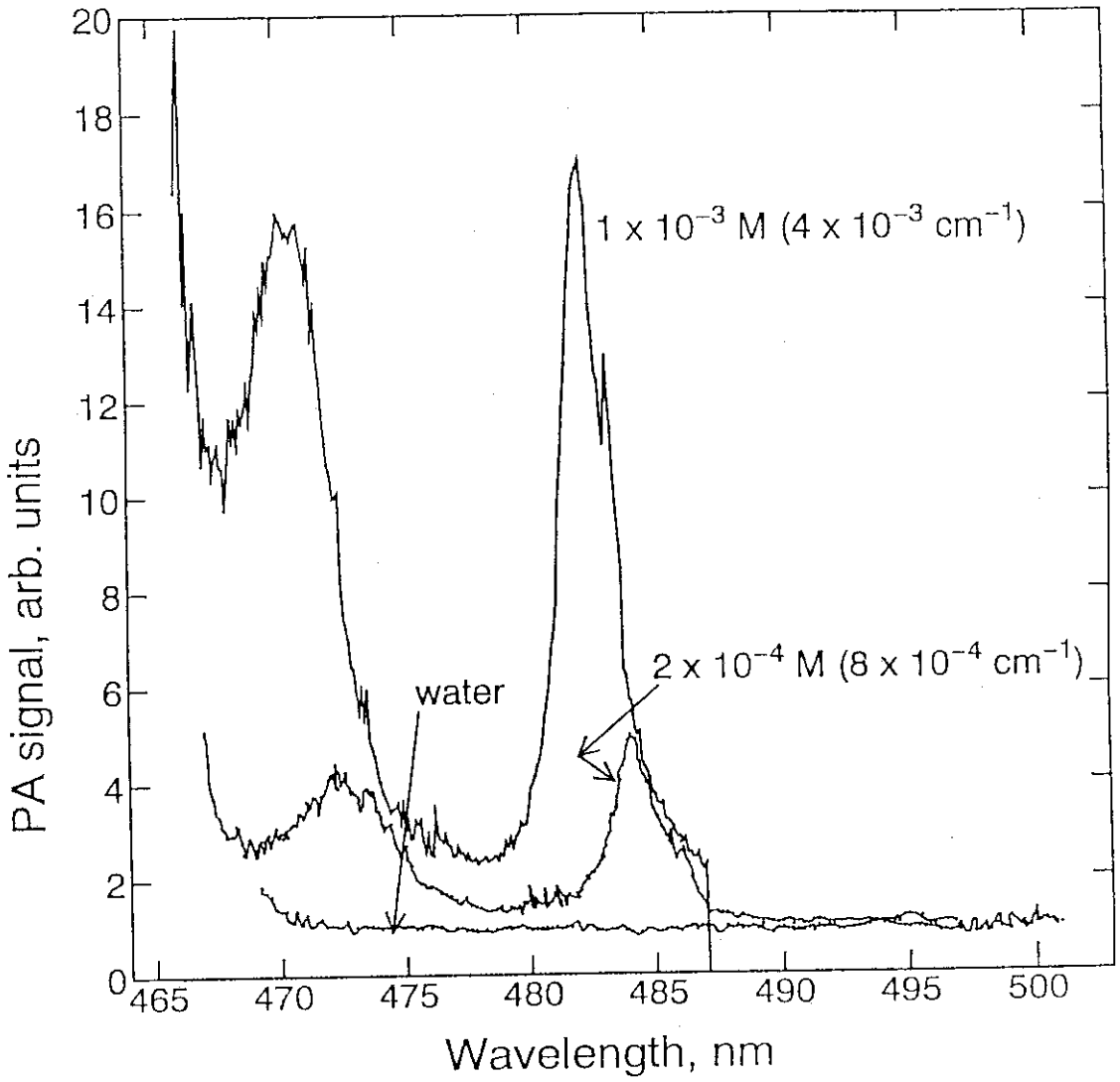

Fig. 15 Photoacoustic spectra of Pr(Ⅲ) solution

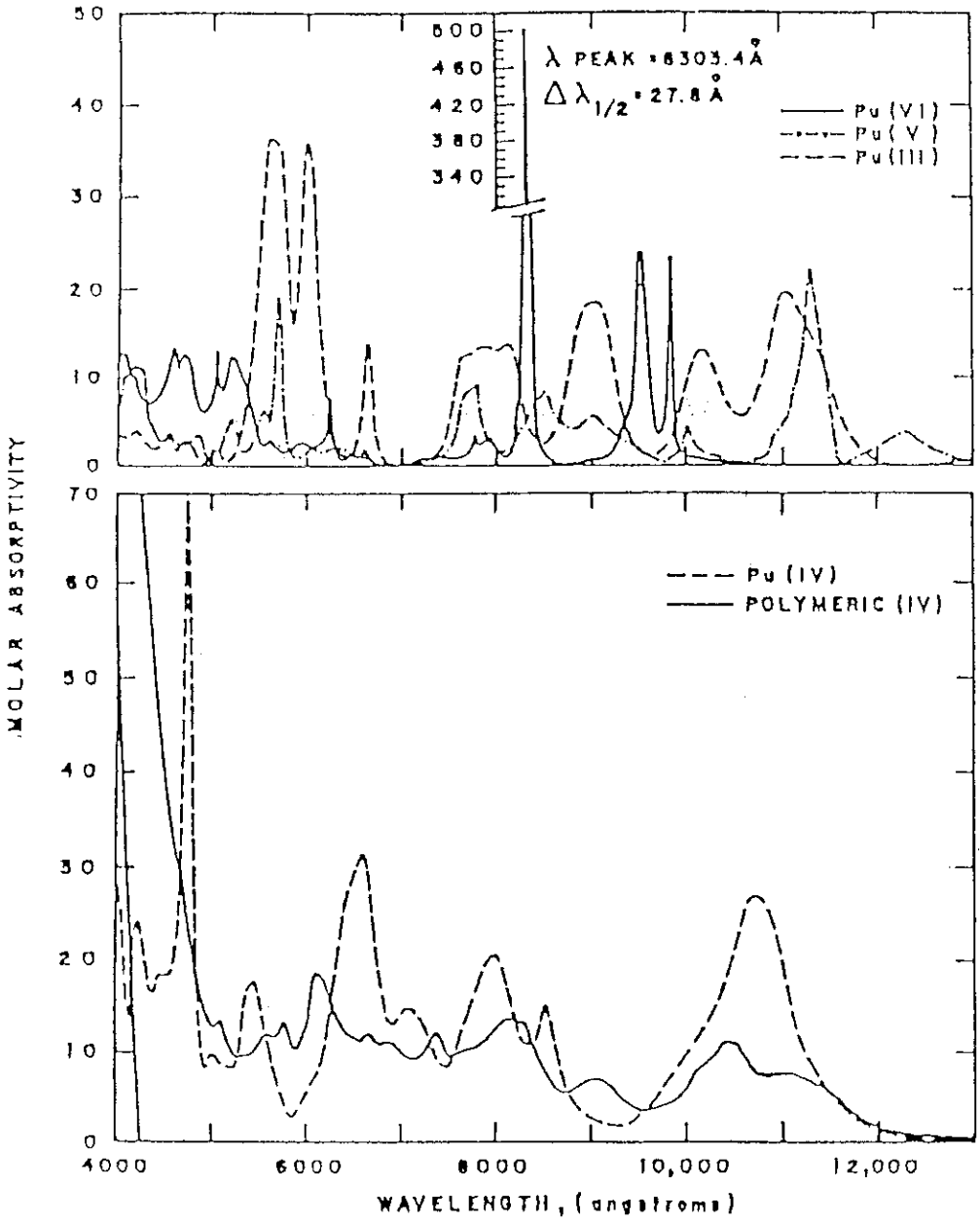

Fig. 16 Absorption spectra of Pu(Ⅲ), Pu(Ⅳ), Pu(Ⅴ), Pu(Ⅵ) and polymeric Pu(Ⅳ) [7] Media : Pu(Ⅲ), Pu(Ⅳ), Pu(Ⅵ)-1M HNO_3 ; Pu(Ⅴ)-1.0M $HClO_4$; polymeric Pu(Ⅳ)-0.2 M HNO_3

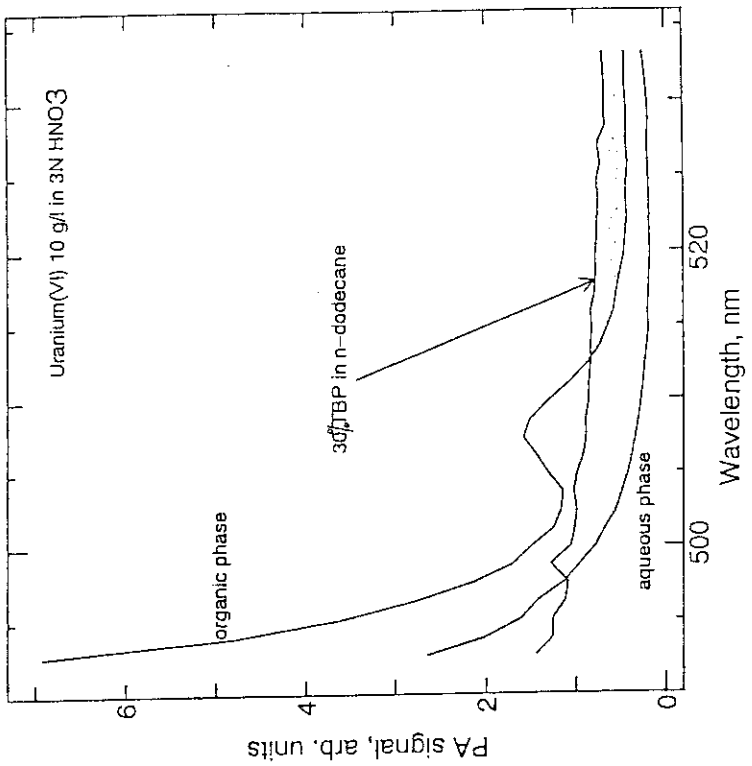

Fig. 18 PA spectra of U(VI) in aqueous phase and in organic phase (30%TBP in n-dodecane)

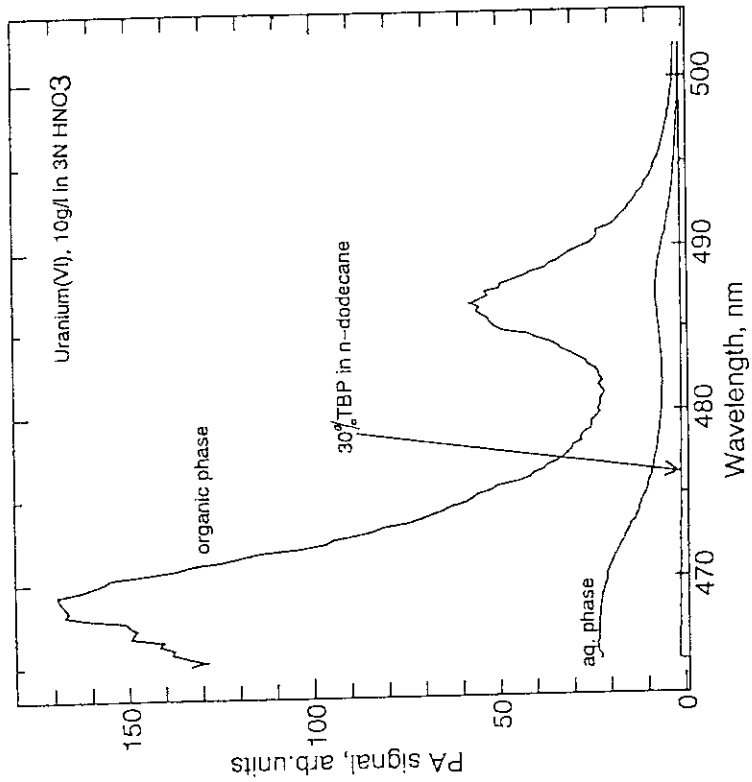

Fig. 17 PA spectra of U(VI) in aqueous phase and in organic phase (30%TBP in n-dodecane)

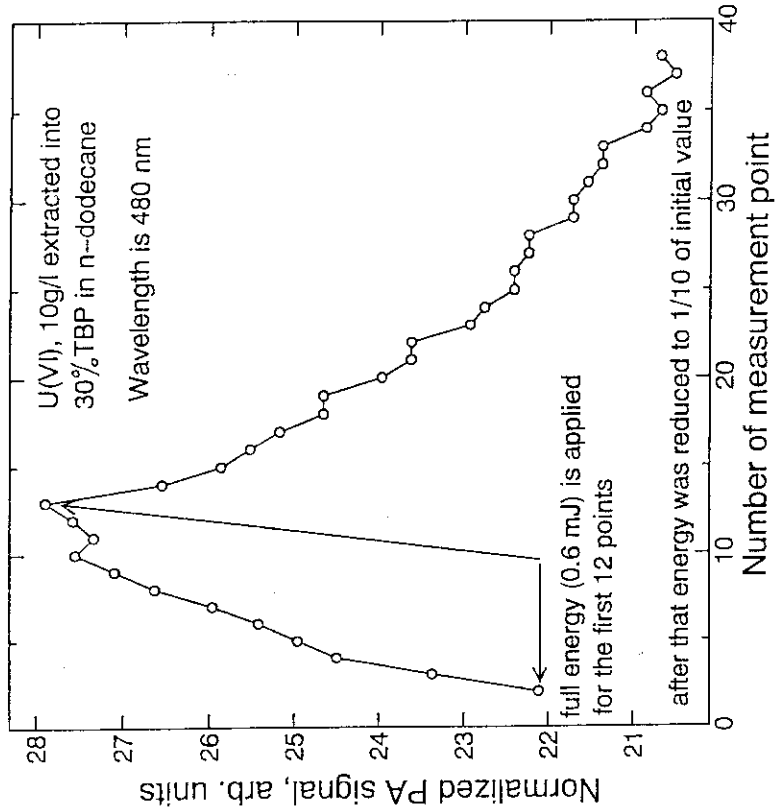

Fig. 19 Illustration of a PA signal drift as result of heat release in the strongly absorbing solution

APPENDIX 1

Modified sample preparation procedure for PAS calibration experiment

Usually for evaluation of such characteristics of a PA spectrometer as its sensitivity and detection limit it is necessary to investigate a dependence of the magnitude of PA signal from the optical density of solution at the selected wavelength corresponding to absorption peak of the species of interest. For this purpose a number of solutions must be prepared covering an appropriate range of the species concentration and calibration experiment is to be conducted which consists in successive measurement of each sample after removing the previously used solution, rinsing the cell, and refilling it with a new portion of the solution going next. Normally a spent portion of the calibration solution is wasted rather than returned to the main supply of this solution in order to avoid any uncontrolled contamination or change of optical characteristics of the solution representing this concentration point to make sure that essentially the same solution can be used for future calibration experiments. This wasting procedure creates no serious problem if the low cost and non hazardous chemicals are used as the background absorbing components or absorbing species itself is not valuable or expensive. But in case of PAS application for detection and determination of radioactive species in nuclear fuel cycle technology all these problems become essential and a care must be taken to reduce amount of radioactive wastes and to save some valuable components used for preparation of a calibration series in PA experiment.

Rather obvious approach to solution of this task may consist in using a single portion of starting (background) solution which is placed into a PA cell and absorbing species is introduced as a little amount of its stock solution directly to cell followed by the measurement of this newly formed solution after the careful mixing of an additive with a matrix. Repeating this procedure several times it is possible to create as many concentration points as necessary to investigate the linearity of PA signal versus the concentration of absorbing component.

However, as it was shown in our previous experiments, the magnitude of PA signal is a very sensitive function of the laser beam position with respect to upper and lower borders of solution inside the PA cell or, in other words,. it is a function of the amount of solution in the cell. That is why it is very important to keep amount of solution constant for all concentration points in the process of PA cell calibration. From the first glance, it is very easy to overcome this difficulty by removing the same amount of solution from the cell prior to introduction of the absorbing species solution. This procedure allows indeed to keep the total solution volume constant throughout the whole calibration experiment, but it creates one more problem: it is clear that starting from the second step of this removal-adding procedure some amount of absorbing component which was contained already in the cell as result of the previous (first) insertion and

mixing step would be lost also in a process of the second removing step. Of course, this drop of concentration may be much low in comparison with the two-fold concentration increase as result of insertion of the second portion of absorbing solution, but if the purpose is to achieve a good linearity of the calibration curve and attain the detection limit of 1.2–1.5 x 10^{-5} cm^{-1}, all, even very minor, controllable sources of uncertainties must be taken into account.

For general mathematical description of concentrational changes occurring in the process of the removal–adding calibration procedure determine the following variables:

V – total volume of solution in PA cell;

v – volume of solution containing the absorbing species, used for creation of concentration increment at the n–th step of calibration procedure;

CC_n – correction coefficient accounting for all previous ((n–1), (n–2), ...,2) negative changes of concentration of the absorbing solute due to its loss with removed portions of solution in PA cell; $C_n = CC_n*C_1$

C_n – concentration of absorbing species in a PA cell solution after the n–th step of the concentrational incrementation procedure.

Let us take for simplicity that v does not depend from n, i.e. essentially the same amount of absorbing stock solution is used in all steps of its introduction into the cell.

After designation of these variables it is clear that the problem is to calculate CC_n for the given v/V ratio and the number of incrementation step.

It is easy to show that $C_2 = C_1*(1 + (1 - v/V)$, therefore, $CC_2 = 1 +(1-v/V)$. The same consideration for C_3 gives $C_3 = C_1*(1+ (1+(1-v/V))*(1- v/V))$, i.e. $CC_3 = 1 + (1+(1-v/V))*(1-v/V)$. The complexity of expression for CC_4, CC_5 and higher members of this row grows rapidly with the value of n, but the general tendency is clear and it allows to find out very simple expression connecting CC_n with $CC_{(n-1)}$:

$CC_n = 1 + CC_{(n-1)}*(1 - v/V)$

This simple recurrent formula can be easily used for calculation of all necessary correction coefficients for the given values n, v and V.

Thus, if A_{init} – is optical density of the absorbing species stock solution, then $A_n = A_{init}*(v/V)*CC_n$, where A_n – is optical density of a calibration solution after the n–th incrementation procedure.

Table 1 shows some results of the CC_n calculation for two different v/V ratios. In both cases a total volume of solution in the PA cell was taken to be equal 2,500 mcl. First line in each row refers to v = 20 mcl increment per one step of the concentration increase, while the second line corresponds to the volume increment of v = 100 mcl.

It is important to emphasize here that a stock solution of absorbing species for this kind of PAS calibration experiment must be prepared using the same background

components which are contained in the medium to be used for PAS application. For example, if it is planned to investigate a possibility of PAS detection of Pu(IV) species in a $UO_2(NO_3)_2$ background solution in 3N HNO_3 the stock absorbing solution of Pu(IV) species (or solution of some sumulated species with the similar absorption band maximum position) must be prepared not in water or in 3N HNO_3 only, but in $UO_2(NO_3)_2$ solution in 3N HNO_3 with the same uranium concentration. This will allow to avoid any dilution of matrix components in the process of calibration experiment keeping the main physical characteristics of solution constant throughout the whole procedure.

APPENDIX 2

Problem of correspondence of an indicated wavelength value to the actual wavelength measured by a monochromator

The wavelength unreproducibility of a TDL-50 laser in the wavelength scanning experiment represents a serious problem for effective PAS application that prompted us to start more detailed investigation of this trouble. First of all a monochromator was installed on the way of the laser beam propagation and a Coumarine-480 gain profile has been explored many times to accumulate enough data for making definite conclusions. The first problem encountered with in the way of this test was related to accidental shift of actual wavelength against its value indicated on the laser wavelength control panel. This event occurred often while fast wavelength rewind from a longer wavelength to a shorther one and each time the magnitude of the shift had a different value, i.e. it was essentially unreproducible.

Another problem, which was discovered in the process of normal (forward, small incremented) wavelength scanning can be expressed as an excessive compression of the laser wavelength scale. Fig. A2 gives an illustration of this effect. The experiment it is derived from was conducted as follows: 1) laser was tuned to the maximum energy output of Coumarine-480 dye, this wavelength was verified by a monochromator and was input into the memory of the laser wavelength controlling unit (thus, at this particular point actual and indicated wavelengths have the same value, i.e. coincide); 2) a 465 nm value (which approximately corresponds to starting point of the dye gain) was input as an initial wavelength and laser was run to this point through a fast rewinding mode.
3) At this new point the real wavelength value was measured again, laser scanning system was run forward with a 5 nm increment and this procedure was repeated several times after each scanning run up to 495 nm (by the laser scale) where the dye generation efficiency dropped below 5% of its maximum output. Therefore, two sets of data have been acquired: wavelength values as indicated by the laser scanning unit (X-axis on Fig. A2) and corresponding to them actual wavelength values measured by a monochromator (Y-axis on this figure). In case of normal laser scanning performance this dependence should be represented by a straght line with a slope equal 1, which means that at any wavelengh point the laser control board indicates true value. In reality, this dependence has a slope of 1.21 or, in other words, laser wavelength indication scale is 21% compressed with respect to actual scale.

It is difficult to say now when and as result of what trouble this compression took place. Fortunately, this effect is reproducible and it is not so difficult to correct a wave-

length scale before plotting the spectra using two parameters: a) exactly measured wavelength difference between actual and indicated value for at least one particular wavelength (it is more convenient to measure this difference at the shorter end of a spectrum to be recorded) and b) scaling coefficient which is found to be 1.21 for the given spectral region.

This correction can be expressed by the following formula:

$$WL_{actual}(i) = WL_{lo} + WL_{m-l} + i * WL_{inc} * SC$$

where $WL_{actual}(i)$ – corrected (actual) wavelength after performing the i–th incrementation procedure;

WL_{lo} – starting wavelength as indicated by a laser control panel;

WL_{m-l} – a monochromator–laser difference value of WL_{lo};

i – number of step in incrementation procedure;

WL_{inc} – wavelength increment, nm;

SC – scaling coefficient, SC = 1.21 in the region of C–480 generation

The results of this research have made it possible now to understand and explain the distorted wavelength distances between the peaks of Nd(III) and Pr(III) on their PA spectra, but as far as the value of WL_{m-1} was not measured during that scanning experiments no correction can be done now for these spectra.

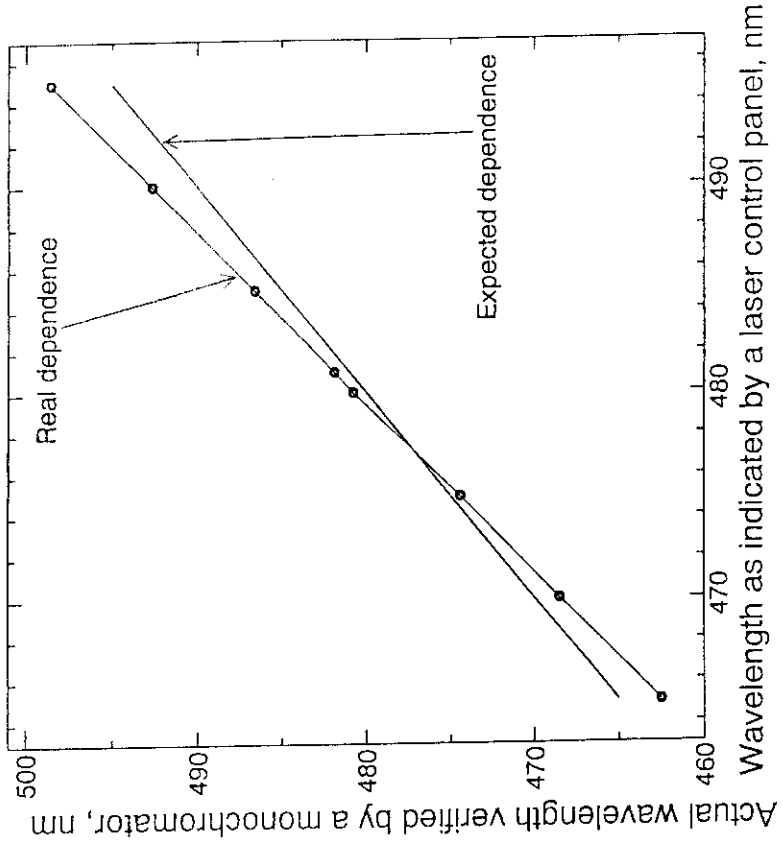

Fig. A2 A TDL50 wavelength scanning characteristic